Beclin1 Regulates Adult Hippocampal Neurogenesis

Michael F. Vaculik

Thesis submitted to the
Faculty of Graduate and Postdoctoral Studies
in partial fulfillment of the requirements
for the Master of Science degree in Neuroscience

Department of Cellular and Molecular Medicine

Faculty of Medicine

University of Ottawa

Abstract

Adult neurogenesis is a process that produces neurons in the adult brain and garners potential for the development of novel therapeutic interventions to combat neurodegenerative and other brain related diseases. With the hope of increasing neurogenesis, active investigations are defining the cellular and molecular mechanisms that regulate adult neural precursor cell (NPC) survival, and thus maintain neurogenesis. Recently, autophagy, an intracellular recycling pathway, has been implicated in regulating adult NPCs in embryonic knockout mice models. Whether autophagy has a similar effect within the adult and how autophagy regulates development of adult NPC remains unknown. Here, we investigate the role of Beclin1, a gene responsible for autophagy induction, in adult hippocampal NPC function in mice. Retroviral-mediated removal of Beclin1 from proliferating adult NPCs *in vivo* led to a reduction in the survival of adult-born neurons. In addition, Beclin1 was removed specifically from nestin-expressing adult neural stem- and progenitor-cells through the development of a Beclin1 nestin-inducible knockout mouse. Beclin1 nKO mice had a reduction in NPC proliferation and development, and overall fewer adult-generated neurons. Together, these findings reveal Beclin1 is required for adult hippocampal neurogenesis through regulating the proliferation and survival of the NPCs, in the absence of changing NPC fate.

Table of Contents

List of Tables

List of Figures

List of Abbreviations

ABC	Avidin-biotin complex
AC3	Activated caspase 3
Atg	Autophagy related gene
Bcl-2	B-cell lymphoma-2
Beclin1	Bcl-2-interaticng myosin-like coiled-coil protein
Beclin1 nKO	Beclin1 nestin-inducible knockout mouse
BLBP	Brain lipid-binding protein
BrdU	5-bromo-2'-deoxyuridine (thymidine analogue)
Cre	Cre recombinase
DAB	Diaminobenzidine
DAPI	4’,6-diamidino-2-phenylindole dihydrochloride
DAPK	Death-associated protein kinase
DCX	Doublecortin
DG	Dentate gyrus
DNA	Deoxyribonucleic acid
dpi	days post injection
ER	Estrogen receptor
ER^{T2}	Estrogen receptor (human T2 mutant)
FACS	Fluorescence-assisted cell sorting
fBeclin1	Floxed Beclin1 mouse
FIP200	200 kDa focal adhesion kinase family interacting protein
GABA	γ-aminobutyric acid
GAD67	67 kDa glutamic acid decarboxylase
GFAP	Glial fibrillary acidic protein
GFP	Green fluorescent protein
HCl	Hydrochloric Acid
IHC	Immunohistochemistry
IP	Intraperitoneal
IPC	Intermediate progenitor cell
JNK1	c-Jun N-terminal kinase 1
KO	Knockout (gene silencing)
loxP	Locus of crossover in P1
mTOR	Mammalian target of rapamycin
ML	Molecular layer
NDS	Normal donkey serum

NeuN	Neuronal nuclear protein
NPC	Neural precursor cell
OB	Olfactory bulb
PBS	Phosphate buffered saline
PCR	Polymerase chain reaction
PEI	Polyethylenimine
PI(3)K	Class III phosphatidylinositol 3-kinase
PI(3)P	Phosphatidylinositol 3-phosphate
PSA-NCAM	Polysialated form of neural cell adhesion molecule
PVI	Parvalbumin-expressing interneuron
R26R-eYFP	Rosa26R-eYellow fluorescent protein
RGL	Radial glia-like cell
RT	Room temperature
SDS	Sodium dodecyl sulfate
SEM	Standard error of the mean
SGZ	Subgranular zone
Sox-2	SRY-related HMG-box gene 2
SVZ	Subventricular zone
TAM	Tamoxifen
TBS	Tris-buffered saline
VPS	Vacuolar protein sorting
WT	Wild type
YFP	Yellow fluorescent protein

Acknowledgements

First and foremost, I would like to thank my supervisor, Dr. Diane Lagace, for granting me with this invaluable learning opportunity and welcoming me into her laboratory, first as an honours student, and again as a graduate student. Theses past few years have been, unquestionably, of the upmost importance in my life. Through your guidance, patience, support, and friendship, I have developed tremendously as a student and a scientist, and I have contributed scientific knowledge that I am very proud of. Your sincere mentorship has also allowed me to excel academically and instilled a great appreciation for scientific discovery. Additionally, your passion, determination, and accomplishments continuously inspire me in the pursuit of personal ambitions. As a result, this experience has helped to shape a future that I could not be more excited for. Thank you.

I would also like to extend a sincere thank you to my thesis advisory committee, Dr. Derrick Gibbings and Dr. Johnny Ngsee for their valuable insight and advice throughout my Masters degree. And of course, thank you to all members of the Lagace lab, including Jagroop Dhaliwal, Maheen Ceizar, Karah Lee, Keren Leviel Kumar, Timal Kannangara, Angela Nguyen, Matthew Seegobin, and Mirela Hasu. You have been outstanding friends and coworkers, provided valuable guidance and technical assistance, and most importantly you have helped to create the wonderful learning environment that is the Lagace lab. These last two years have been nothing but a blast and I will always cherish the memories.

Last, but not least, I would like to thank my close friends and family for their constant support throughout all of my endeavors. Accomplishments like this would not be possible without you.

Introduction

1.1 Adult Neurogenesis: The Discovery

The discovery of adult neurogenesis marked the beginning of a paradigm shift in our contemporary understanding of brain plasticity (Gross, 2000). At the turn of the 20th century, it was universally accepted that the brain was structurally static, a characteristic thought to be necessary in maintaining stability of complex neural circuits and the elaborate architecture of the brain. It was not until half a century later that this notion was challenged by Joseph Altman and colleagues, who found actively proliferating cells in the adult rat brain that could be labeled with a thymidine analogue and become mature adult-generated neurons (Altman, 1962; Altman and Das, 1965; Altman, 1969). Altman further identified adult-generated neurons were mainly localized to the dentate gyrus of the hippocampus and the olfactory bulb and hypothesized their role in memory. Altman's seminal findings were largely ignored and the dogma of a static brain persisted until three decades later, when Eriksson and colleagues identified adult-born neurons in the post-mortem human brain (Eriksson et al., 1998; Kaplan, 2001). This generated excitement and future investigations due to the prospect of promoting the proliferation and survival of the endogenous adult-generated neurons in the brain as a novel therapeutic target for the treatment of brain disorders.

Since the early discoveries of Altman, there have been significant advancements in our understanding of the development, regulation, and function of newborn adult neurons (Aimone et al., 2014; Christian et al., 2014). These findings have been possible through methodological improvement in experimental techniques, and particularly in our ability to permanently label and trace the dividing neural precursor cells (NPCs). For instance,

the development of the synthetic thymidine analogue 5-bromo-3'-deoxyuridine (BrdU), which incorporates into the DNA of proliferating cells allowed NPCs to be birthdated and visualized through immunohistological (IHC) methods (Gross, 2000). Fred Gage's group was the first to use BrdU and demonstrate in many seminal papers the regulation of adult neurogenesis in rodents by various physiological factors including stress, age, exercise, and environmental enrichment (Kuhn et al., 1996; Kempermann et al., 1997; van Praag et al., 1999). The developing NPCs could also be fate mapped by identification of the BrdU-labeled cells with transient proteins that are endogenously expressed at specific developmental stages of neurogenesis. For example, BrdU cells that also express nestin are often labeled as stem or progenitor cells (Lendahl et al., 1990). Other proteins such as doublecortin (DCX), which is expressed in immature neurons that develop from NPCs, can also be labeled through IHC methods (Brown et al., 2003). The specificity of these proteins to the NPCs and their progeny also provided a means to create several transgenic reporter mice (Dhaliwal and Lagace, 2011). For example, the nestin-GFP reporter mice allowed for isolation and population analysis of nestin-expressing NPCs within the adult brain (Yamaguchi et al., 2000; Dhaliwal and Lagace, 2011).

Although the reporter mouse models allowed for visualization of developing NPCs, they are limited by the temporal control of expression of the florescent label (Dhaliwal and Lagace, 2011). This limitation was overcome with the introduction of conditional transgenic mice using a Cre-loxP system and other similar technology. In the case of the Cre-loxP system, Cre recombinase is under the control of a transiently activated promoter and when combined with the floxed fluorescent reporter mouse the result is permanent fluorescent labeling and fate mapping of populations of cells. For instance, the creation

of a glial fibrillary acidic protein (GFAP) driven Cre mouse led to a seminal report that identified GFAP expression in stem-like NPCs and fate-mapped their development in the dentate gyrus (Garcia et al., 2004). Further enhanced temporal control was then gained through the introduction of inducible transgenic models that are created by fusing Cre to an estrogen receptor (ER), allowing for the activation of Cre activity upon administration of an estrogen ligand such as tamoxifen (TAM) (Imayoshi et al., 2006; Lagace et al., 2007). The power of this methodology is that TAM can be given at any time during development allowing for studies to fate-map or alter gene expression specifically in adult neurogenic cells. Similarly, the application of retroviral-mediated gene transfer in combination with Cre-loxP technology, offers the ability to target specifically adult NPCs and thus is another powerful alternative to BrdU and complex transgenic models in birth-dating and fate-mapping developing NPCs (van Praag et al., 2002; Zhao et al., 2006). Lastly, the use of Cre-loxP technology in retroviral-mediated gene transfer in conditional and inducible mouse models permitted new methods of investigating the cellular and molecular mechanisms that regulate NPCs through targeted gene ablation (Tashiro et al., 2006a; Dhaliwal and Lagace, 2011). Overall, the development of these techniques and transgenic models within the last two decades have allowed for a heightened understanding of the NPC lineage and its progeny in the adult brain.

1.2 Overview of the Birth and Development of Adult-Born Neurons

Adult neurogenesis encompasses three essential processes that are critical to the overall level of neurogenesis: cell proliferation, neuronal differentiation, and cell survival (Aimone et al., 2014). The NPCs that given rise to adult-born neurons populate two regions of the adult brain including the subventricular zone (SVZ) of the lateral ventricles

and the subgranular zone (SGZ) of the dentate gyrus, where they produce olfactory bulb neurons and hippocampal granule neurons, respectively (Zhao et al., 2008; Ming and Song, 2011). The SVZ and SGZ represent the neurogenic niches or specialized microenvironments containing microglia, astrocytes, and vasculature that permit, regulate, and support adult neurogenesis (Aimone et al., 2014). Since this thesis studies adult hippocampal neurogenesis, the following sections will focus on development of NPCs in the dentate gyrus.

The neurogenic cells in the SGZ are categorized into developmental stages by cell morphology, expression of specific transient endogenous cell markers, and electrophysiological properties (Aimone et al., 2014; Christian et al., 2014). Although various nomenclature have been used to describe NPCs throughout their development, this thesis uses the most prominent classification system first proposed by Gerd Kempermann (Kempermann et al., 2004). As shown in Figure 1, adult-born hippocampal neurons arise from a population of adult neural stem cells in the SGZ. The *in vivo* multipotent self-renewing adult neural stem cells, or Type-1 cells, are the nestin and GFAP expressing radial glia-like cells (RGLs) (Bonaguidi et al., 2011; Encinas et al., 2011; Bonaguidi et al., 2012). Although another model proposed a subpopulation of sex determining region Y-box 2 (Sox2) expressing non-radial cells as the Type-1 cells, *in vivo* evidence suggests these cells have only limited self-renewal and unipotent differentiation (Suh et al., 2007; Lugert et al., 2010; Bonaguidi et al., 2012). The RGLs possess triangular soma and a long apical process that extends through the granule cell layer and sprouts into bushy processes with vascular end feet in the molecular layer as

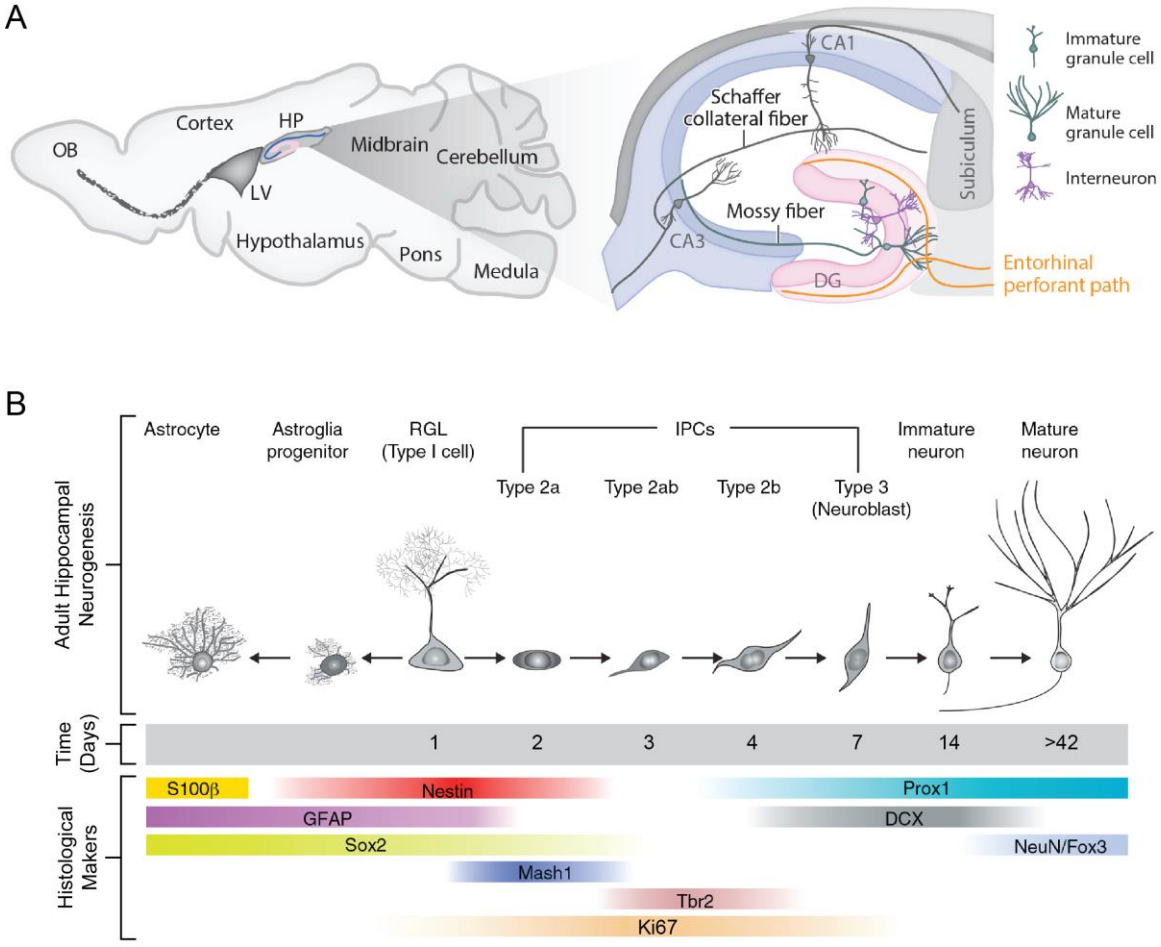

Figure 1. Adult neurogenesis in the SGZ of the hippocampal dentate gyrus. A) A sagittal section of an adult mouse brain highlighting the location of the hippocampus (HP) where adult neurogenesis produces new granule neurons in the dentate gyrus (DG) that receive synaptic inputs from the entorhinal perforant path, and provide outputs along the mossy fiber pathway to pyramidal neurons in the CA3. **B)** Summary of the developmental process of adult hippocampal neurogenesis, including a time course of morphological development and histological marker expression. LV, Lateral Ventricles; OB, Olfactory Bulb. Modified from: Bonaguidi et al. (2012) and Christian et al. (2014).

first visualized through the use of the nestin-GFP reporter mouse (Yamaguchi et al., 2000; Filippov et al., 2003). Although the RGLs share similar morphological and electrophysiological properties to astrocytes, they do not express the astrocyte specific cell marker S100β, nor do astrocytes express nestin, and therefore the RGLs are considered a distinct cell population (Filippov et al., 2003). The RGLs have also been identified through their expression of brain lipid-binding protein (BLBP) and Sox2, however these markers are not exclusive to Type-1 cells, highlighting the need for identifying RGLs with GFAP and another ubiquitous histological marker (Duan et al., 2008; Ming and Song, 2011). Unlike the putative neural stem cells in the developing brain, RGLs are largely quiescent, accounting for just ~5% of divisions yet comprising two-thirds of the nestin-expressing cell population (Kronenberg et al., 2003). Once activated RGLs divide symmetrically or asymmetrically before returning to quiescence (Bonaguidi et al., 2011) or can directly differentiate into a GFAP expressing astroglia without dividing (Brunne et al., 2010). The frequency of symmetric divisions, which results in two RGLs, is relatively low when compared to the rate of asymmetric divisions that result in one RGL cell. In addition to the RGL cell, an asymmetric division produces either a neurogenic Sox2-expressing intermediate progenitor cell (IPC), or a GFAP-expressing bushy astroglia. Therefore overall a RGLs can make any one of these four fate decisions through multiple rounds of cell division and the total population of RGL reflects the summation of fate decisions of the RGL cells over time: maintenance through quiescence or asymmetric self-renewal, reduction through terminal astrocytic differentiation, or expansion through symmetric self-renewal (Bonaguidi et al., 2011). Although the mechanisms that regulate RGL fate decision are not fully understood,

recent evidence demonstrates that RGL quiescence can be controlled by parvalbumin-expressing interneurons (PVIs) (Song et al., 2012). RGLs respond to the neurotransmitter γ-aminobutyric acid (GABA) released from terminal ends of PVIs expressing the 67 kDa glutamic acid decarboxylase (GAD67). PVIs can also promote RGL quiescence, indicating local neural circuitry can regulate RGL fate decisions, and likely contribute to the overall regulation of adult neurogenesis.

IPCs are the non-radial, unipotent, and self-renewing NPCs of the neuronal lineage. The IPCs are rapidly proliferating with an average cell cycle length of approximately 12-24 hours (Mandyam et al., 2007). As a result, all IPCs express proliferating markers including Ki67, and they are the population of cells prominently labeled by BrdU (Kronenberg et al., 2003), and retroviruses (van Praag et al., 2002; Jagasia et al., 2009). IPCs have been characterized to proceed through three developmental stages called type-2a, type-2b, and type-3 (Kronenberg et al., 2003; Kempermann et al., 2004), as classified by marker expression and morphology. For instance, type-2a cells have a dense irregular nucleus and begin to form short processes that are oriented tangentially to the granule cell layer, whereas type-2b cells have marginally longer process that begin to orient laterally to the granule cell layer (Kronenberg et al., 2003; Kempermann et al., 2004). Type-2a cells can also be identified through their expression of nestin, whereas type-2b cells express both nestin and the immature neuronal marker DCX. Type-3 cells have a rounded nucleus with longer apical processes that begin to extend through the granule cell layer towards the molecular layer. The type-3 cells do not express nestin, and are often identified through their expression of DCX. Additionally these cells can be identified by the expression of other markers indicative of neuronal differentiation, such

the polysialated form of neural cell adhesion molecule (PSA-NCAM), and calretinin (Brandt et al., 2003; Kempermann et al., 2004).

Progression through the three IPC developmental stages occurs rapidly, and just one week after birth, type-3 cells undergo terminal differentiation to form post-mitotic immature neuron (Kempermann et al., 2004; Aimone et al., 2014). Immature neurons develop physiologically and morphologically for approximately 3 weeks (4 weeks post-birth) until they cease to express DCX, initiate NeuN expression, and exhibit a neuronal phenotype with pronounced apical dendrites and mossy fibre axons (Aimone et al., 2014). The immature neuron axon, also called mossy fibres, reach the CA3 region at about two weeks of age, even before the first dendritic spines are detected (Zhao et al., 2006). The apical dendrites develop into the molecular layer where arborisation and dendritic spine density significantly increases between 2.5 and 4 weeks of age (Zhao et al., 2006). This maturation process is hypothesized to allow the immature neurons to form neural connections in the entorhinal perforant path and integrate into existing neural networks, and thus marks a critical stage in their survival (Kuhn et al., 2005; Tashiro et al., 2007). New adult-born neurons will continue to mature and express NeuN and calretinin, as well as receive input from the entorhinal perforant path and send excitatory outputs along the mossy fibre pathway to pyramidal cells in the CA3 region of the hippocampus. Although many of these histological and morphological characteristics of the cells are present by 4 weeks of age, the cells are not indistinguishable from the resident granule neurons in terms of electrophysiological properties until about 6-8 weeks of age (van Praag et al., 2002; Zhao et al., 2006).

Interestingly, of the thousands of NPCs that are generated in the adult brain each day, almost 80% undergo apoptosis during maturation (Kuhn et al., 2005; Sierra et al., 2010). This paradox raises an outstanding question in the field of adult hippocampal neurogenesis: what cellular and molecular processes regulate the survival of developing NPCs? It is conceivable that enhancing the production of adult-born neurons in the brain is a mechanism by which future regenerative medical therapies could be developed. Recent evidence has begun to unravel how the regulation of adult neurogenesis is executed by complex intrinsic and extrinsic cellular and molecular mechanisms involving numerous transcription and epigenetics factors, local paracrine signaling and communication with the existing neuronal networks (Hsieh, 2012; Aimone et al., 2014; Yao and Jin, 2014). Given the involvement of adult neurogenesis in numerous physiological processes, and its potential in future regenerative medical therapies, it is imperative that the mechanisms regulating the survival of the NPCs and its progeny are well defined. This thesis addresses this need by exploring the role of the autophagy regulator Bcl-2-interaticng myosin-like coiled-coil protein (Beclin1) in adult hippocampal neurogenesis.

1.3 A Role for Autophagy in the Survival and Development of Neurons

Macroautophagy (hereafter referred to as autophagy) is defined as an intracellular recycling pathway responsible for the degradation of cellular constituents (Mizushima and Komatsu, 2011; Boya et al., 2013). Autophagy is present in many tissues throughout the body and has a fundamental physiological function in maintaining cellular homeostasis and protecting cells from various insults, including miss-folded proteins, damaged organelles, and varying nutrient availability. The major cellular process of

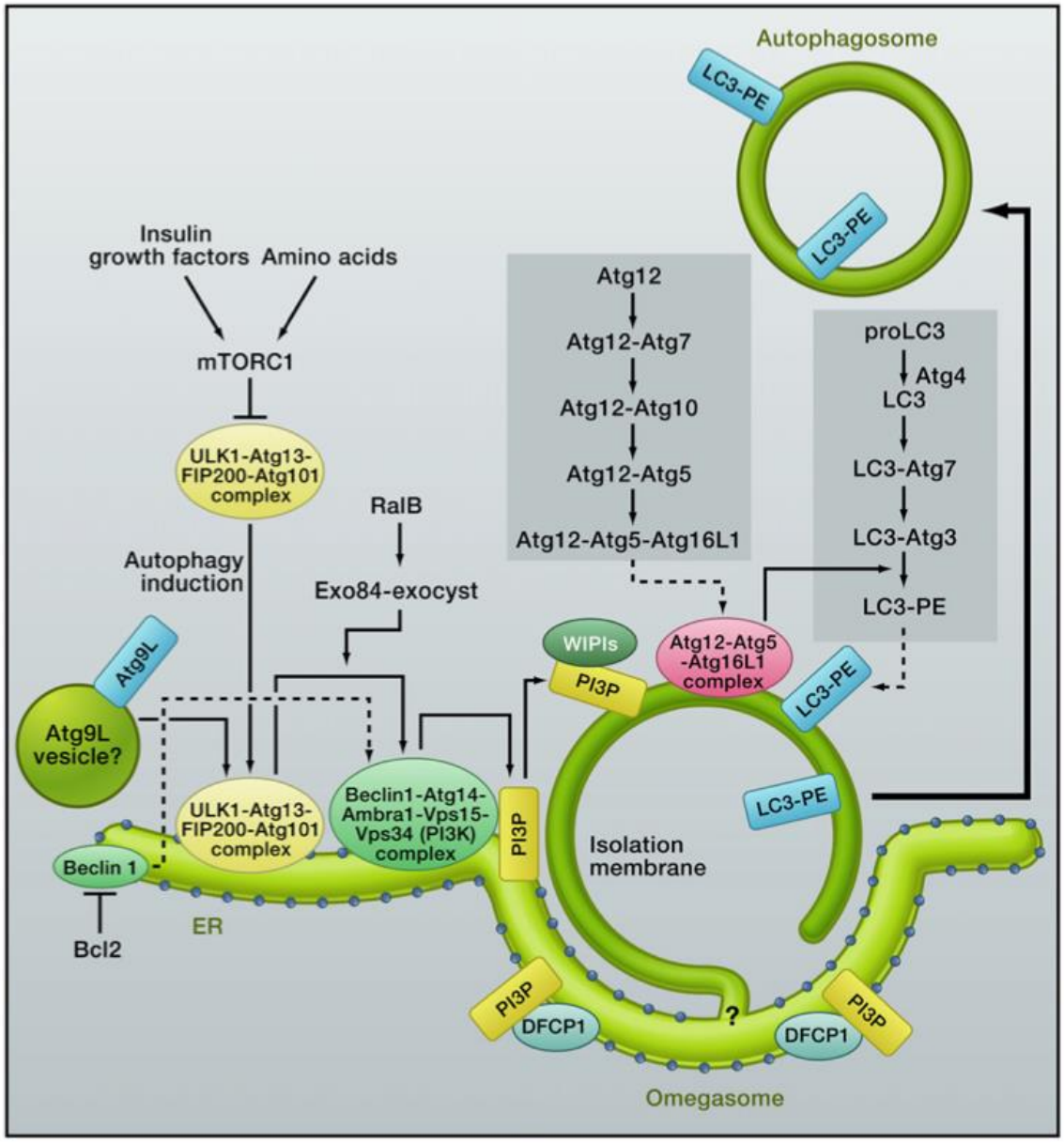

Figure 2. The autophagy pathway. The autophagy pathway consists of more than thirty genes, and has two major regulatory players. The first, mTORC1, acts to inhibit autophagy in the presence of nutrients and absence of stressful stimuli. The second, Beclin1 induces autophagy upon release from Bcl-2 by activating PI3P activity through the formation of the core complex**.** Modified from Mizushima and Komatsu (2011).

autophagy is shown in Figure 2 and consists of autophagosome formation, engulfment of targeted cellular constituents, and degradation of the autophagosome via lysosomal fusion. Autophagy was first discovered to be more active under conditions of starvation and proceeding biochemical studies revealed that autophagy is negatively regulated by the serine/threonine kinase mTOR (mammalian target of rapamycin) (Boya et al., 2013; Yamamoto and Yue, 2014). Together these studies suggest that autophagy is generally a cell-death pathway that functions to provide energy and metabolic precursors under conditions of starvation. However, in many cellular contexts, it has now also been demonstrated that autophagy functions as a cell-survival pathway that can selectively remove and recycle proteins and/or organelles to limit their cumulative deleterious effects (Gordy and He, 2012; Macintosh and Ryan, 2013).

Autophagy has been implicated as a regulator of development due to the substantial cellular remodeling that requires control of protein and organelle turnover during proliferation and differentiation of stem and progenitor cells (Di Bartolomeo et al., 2010; Phadwal et al., 2013). In support of this, autophagy was demonstrated to be critical for embryogenesis with many knockout mouse models showing prenatal (Yue et al., 2003; Fimia et al., 2007; Tsukamoto et al., 2008) or perinatal lethality (Kuma et al., 2004) and neurodegeneration (Hara et al., 2006; Komatsu et al., 2006). *In vitro* evidence has further demonstrated that autophagy was required for normal neuronal differentiation of mouse embryonic olfactory bulb stem cells (Vazquez et al., 2012) and neuroblastoma N2a cells (Zeng and Zhou, 2008). The requirement of autophagy in embryonic development suggests the possibility for a similar requirement in the development of adult stem cells.

Evidence demonstrating autophagy is required within the adult brain is also emerging (Yamamoto and Yue, 2014) as intermittent or short-term fasting and mTOR inhibition can induce autophagy in adult neurons including cortical neurons and Purkinje cells (Alirezaei et al., 2010; Kaushik et al., 2011; Proenca et al., 2013). Furthermore, mechanical stress in adult neurons such as axotomy or nerve crush, excitotoxic stress, and drug-induced toxicity can elicit autophagosome production and accumulation (Yue et al., 2009). In addition, autophagy ablation in Purkinje cells triggers cell-autonomous axonal dystrophy and degeneration of axonal terminals (Komatsu et al., 2007). Thus, these findings support that autophagy is required for axonal maintenance and normal neuronal functioning.

Within the context of adult neurogenesis autophagy has been indirectly implicated in the survival and normal development of NPCs. Wang et al. (2013) first reported that there is a progressive loss of stem cells and abnormal differentiation of NPCs in the adult brain following embryonic ablation of the autophagy gene FIP200 (encoding a 200 kDa focal adhesion kinase family interacting protein). More recently, Yazdankhah et al. (2014) showed heterozygous Beclin1 mice have reduced autophagy and demonstrate a role for Beclin1 in the proliferation of NPCs and survival of immature and mature neurons in the SVZ of the adult brain. Together these results both support that removal or reduction in the level of autophagy in the embryonic brain results in a reduction in adult neurogenesis. However, it remains unknown if an inducible removal of autophagy in the specific context of adult neurogenesis would mimic the deficits that are observed following an embryonic knockout. Our laboratory has multiple projects that are addressing this need. We have found that autophagy can regulate the survival of NPCs during adult

neurogenesis using Cre-loxP technology to ablate the autophagy related gene 5 (Atg5) via a retroviral delivery approach (Xi et al., 2015). Additionally, this thesis examines the effect of removal of Beclin1 in adult generated NPCs. We specifically targeted Beclin1 due to critical role of this protein in mediating crosstalk between autophagy and apoptosis (He and Levine, 2010).

1.4 Beclin1: Mediating Crosstalk Between Autophagy and Apoptosis

As its name suggests, Beclin1 was originally discovered not as an autophagy regulator, but as a B-cell lymphoma-2 (Bcl-2) interacting partner (Liang et al., 1998). Subsequent studies demonstrated that Beclin1 could restore autophagic activity in Atg6-disrupted yeast and inhibit tumorigenesis, designating Beclin1 as an autophagy regulator and tumor suppressor gene (Aita et al., 1999; Liang et al., 1999). Similar to other autophagy knockout models, Beclin1 global knockout mice were embryonically lethal due to severe underdevelopment, supporting the role for Beclin1 in embryogenesis (Yue et al., 2003). Beclin1's role as a tumor suppressor gene was further supported by experiments with Beclin1 heterozygous knockout mice. While these mice developed normally, they had an increase in spontaneous tumor formation, indicating that Beclin1 is a haploinsufficient tumor suppressor (Qu et al., 2003; Yue et al., 2003).

These early studies set the stage for research, predominantly in the context of cancer, to elucidate Beclin1 interactors, its role in various molecular pathways, and ultimately how it functions as an autophagy regulator (Funderburk et al., 2010). Briefly, Beclin1 was discovered to initiate the formation a core complex with class III phosphatidylinositol 3-kinase (PI(3)K), the mammalian orthologue of vacuolar protein sorting 34 (VPS34), that is critical in autophagy initiation and vesicle nucleation to form the autophagosome

(Kihara et al., 2001) (Figure 2). Activation of PI(3)K activity by Beclin1 produces phosphatidylinositol 3-phosphate (PI(3)P) and enables the recruitment of other Atg proteins involved in autophagosome biogenesis (Petiot et al., 2000; Kihara et al., 2001). The core complex contains additional Beclin1 interactors including Barkor (mammalian homologue of Atg14L) (Itakura et al., 2008) and Ambra1 (Fimia et al., 2007), as well as the PI(3)K interactor VPS15, all of which aid in targeting the core complex to vesicle nucleation sites and modulate its activity (Wirawan et al., 2012).

Since Beclin1 was originally discovered as a Bcl-2 interactor, it was hypothesized that the Beclin1-Bcl-2 complex could elicit crosstalk between autophagy and apoptosis. In agreement with this hypothesis Bcl-2 negatively regulates autophagy through its direct interaction with Beclin1 as shown in Figure 3 (Pattingre et al., 2005). The interaction between Beclin1 and Bcl-2 is regulated by many mechanisms, including the phosphorylation of Beclin1 by death-associated protein kinase (DAPK) (Zalckvar et al., 2009), or phosphorylation of Bcl-2 by c-Jun N-terminal kinase 1 (JNK1) (Wei et al., 2008), which promotes autophagic activity. Additionally, caspase-mediated cleavage of Beclin1 inhibits autophagy, and the C-terminal cleavage product amplifies mitochondrial-mediated apoptosis through release of pro-apoptotic factors (Djavaheri-Mergny et al., 2010; Wirawan et al., 2010). This molecular crosstalk between the pro-survival autophagic pathway and the pro-death apoptotic pathway function are important in regulating cell survival in a variety of cellular contexts (Maiuri et al., 2007).

Within the adult brain the *in vivo* functional role of Beclin1 had not been explored until recently with the creation of floxed Beclin1 transgenic mice by Dr. Zhenyu Yue (McKnight et al., 2014). Using the floxed Beclin1 they showed that conditional removal

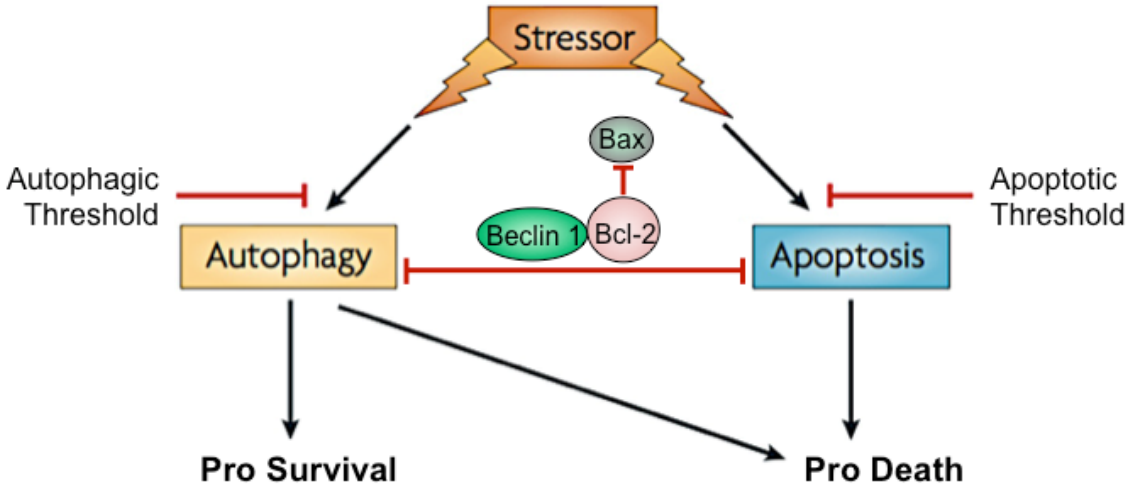

Figure 3. Molecular crosstalk between the autophagic and apoptotic pathway. Beclin1 is an important autophagy regulator located upstream in the pathway where it directly interacts with Bcl-2 and allows for crosstalk between autophagy and apoptosis. Modified from Maiuri et al. (2007).

of Beclin1 from the forebrain of mice during embryogenesis resulted in severe neurodegeneration in the hippocampal CA1 pyramidal cell layer and in the cerebellar Purkinje cell layer at post-natal day 30. These results support that Beclin1 is required for neuronal survival. Interestingly, McKnight et al. (2014) also show a variety of mechanistic evidence to support that neuronal survival is regulated by autophagy and endocytosis, suggesting that Beclin1 acts as a nexus point between autophagy, endocytosis, and apoptosis.

These findings lead us to further question whether in the context of adult neurogenesis removal of Beclin1 would induce a significant reduction in survival that could be attributed to changes in autophagy, endocytosis and, or apoptosis. In order to address this question, I examined the functional role of Beclin1 in adult neurogenesis through removing Beclin1 specifically from adult NPCs using retroviral-mediated gene transfer and creating a Beclin1 nestin-inducible knockout (Beclin1 nKO) mouse.

Objectives and Hypothesis

Objective:

In order to harness the potential of adult neurogenesis for future regenerative medical therapies, it is essential that we understand the cellular and molecular mechanisms that regulate this dynamic process. Autophagy, a cellular recycling pathway, has recently been suggested to regulate adult hippocampal neurogenesis (Wang et al., 2013; Yazdankhah et al., 2014). Beclin1 is an essential autophagy regulator that is involved in crosstalk between the pro-survival autophagic and pro-death apoptotic pathways (He and Levine, 2010). The objective of this thesis to determine whether Beclin1 is regulates the survival and/or development of NPCs during adult hippocampal neurogenesis.

Hypothesis:

Beclin1 regulates the survival, proliferation, and maturation of NPCs during their development in the adult naïve brain.

Aims:

1. Determine whether retroviral-mediated gene ablation of Beclin1 in proliferating NPCs affects survival and development over time.
2. Determine whether removal of Beclin1 from nestin-expressing NPCs and their progeny has effects on NPC survival, proliferation, and development, using a triple transgenic nestin inducible Beclin1 knockout mouse.

Materials and Methods

2.1 Animals

Animal procedures were performed with approval from the University of Ottawa Animal Care Committee and adhered to the Guidelines of the Canadian Council on Animal Care. Transgenic mouse lines used in this study include: floxed Beclin1 (fBeclin1) mice (created by McKnight et al., 2014, obtained from Dr. Zhenyu Yue, Icahn School of Medicine at Mount Sinai); inducible Nestin-CreER^{T2} mice (created by Imayoshi et al., 2006, line 4.1 obtained from Paul Frankland, Hospital for Sick Children); reporter R26R-enhaned Yellow Fluorescent Protein (eYFP) mice (created by Srinivas et al., 2001, obtained from Jackson Laboratory). Inducible Beclin1 knockout (Beclin1 nKO) mice were created by crossing the fBeclin1, Nestin-CreER^{T2} and R26R-eYFP mice as described below. Age-, sex- and littermate-matched control and mutant mice were randomly collected on the basis of their genotype. All strains were obtained and maintained on a C57bl/6J background. Animals were group housed in standard laboratory cages and kept on a 12 hour night/day cycle with ad libitum access to food and water.

2.2 Genotyping

Animals were genotyped at 3 weeks of age through DNA samples obtained from ear clippings (~1 mm^2). DNA was extracted using the HotSHOT methodology (Truett et al., 2000). Briefly, ear clippings were incubated an Alkaline Lysis Buffer (25 nM NaOH and 0.2 mM Na_2EDTA) at 95°C for 30 minutes prior to addition of the Neutralization Solution (40 mM Tris-HCl). Polymerase Chain Reaction (PCR) was completed using primers (Table 1) according to previously published protocols for fBeclin1 (McKnight et

al., 2014), Nestin-CreER^{T2} (Imayoshi et al., 2006), and R26R-eYFP (Srinivas et al., 2001). The resulting PCR products were resolved by size on a 2% agarose gel using electrophoresis. Size of the PCR products was visualized with ethidium bromide staining under ultraviolet light and estimated by comparison with a 100 base pair (bp) DNA ladder (DM001-R500M; Frogga Inc.).

2.3 Retroviral Vectors and Injections

Retroviral vectors *CAG-GFP-Cre* and *CAG-RFP* and corresponding packing envelopes were generously provided from Dr. Fred Gage (Salk Institute of Biological Science). Retroviruses were prepared using a previously published protocol (Tashiro et al., 2006b) with minor modifications by Jagroop Dhaliwal (PhD Candidate in Lagace Lab). Briefly, 293T cells were plated ($8x10^6$ cells/150 mm) and co-transfected using polyethylenimine (PEI, Polyscience Cat# 23966) with either the *CAG-GFP-Cre* or *CAG-RFP* retroviral plasmid combined with the *CMV-Gag-Pol* packing plasmid and *CMV-VSV-G* envelope plasmid in a 3:2:1 ratio, respectively. At 48 and 72 hours post-transfection the supernatant containing the virus was collected and concentrated by two rounds of ultracentrifugation (20,000 RPM for 2 hours at 4°C) with 20% sucrose cushion, dissolved in phosphate buffered saline (PBS). Virus titre was determined by live tittering through infection of 293T cells plated in a 24-well plate (1.25×10^5 cells) with 100 µl of diluted (10^4 dilution) virus. Fluorescence-positive cells were quantified 48 hours post-infection and the number of infectious units (IU) per ml was calculated as the mean of the product of the number of infected cells per viewing field, the well area (243.22 mm^2), and the dilution factor (10^4). Virus titre was approximately 6.7×10^8 IU/ml for the *GFP-Cre* virus and 1.7×10^9 IU/ml for the *RFP* virus.

Table 1. PCR Primers used for genotyping transgenic mice. The control and transgene primer sequences are shown as well as the size of the PCR product obtained from each pair of primers.

Gene		5' Primer	3' Primer	Size (bp)
CreER^{T2}	+Control	P26: 5'–CTAGGCCACAGAATTGAAAGATCT–3'	P27: 5'–GTAGGTGGAAATTCTAGCATCATCC–3'	324
	Transgene	P24: 5'–GCGGTCTGGCAGTAAAAACTATC–3'	P25: 5'–GTGAAACAGCATTGCTGTCACTT–3'	100
YFP	WT	P21: 5'–GGAGCGGGAGAAATGGATATG–3'	P20: 5'–GCGAAGAGTTTGTCCTCAACC–3'	560
	Transgene	P21: 5'–GGAGCGGGAGAAATGGATATG–3'	P19: 5'–AAAGTCGCTCTGAGTTGTTAT–3'	310
fBeclin1	WT	P70: 5'–CCACCACCAAGGCAGCGGGTAG–3'	P69: 5'–TCACTGATGGCTCTAACCTCAACTCGTC–3'	650
	Transgene	P70: 5'–CCACCACCAAGGCAGCGGGTAG–3'	P69: 5'–TCACTGATGGCTCTAACCTCAACTCGTC–3'	850

Retroviruses were injected bilaterally into the dentate gyrus of 7-9 week old mice using stereotaxic surgery. Mice were anesthetized throughout surgery with 2% isoflurane. The mice were injected with either *GFP-Cre* and *RFP* viruses in a 1:1 ratio mixture (volume 1.5 μl) or *GFP-Cre* (volume 1 μl). Injections were administered by microinjection using a 33 gauge (0.21 mm diameter) needle (7803-05; Hamilton), into the dentate gyrus using coordinates of -1.7 mm rostrocaudal and ±1.2 mm mediolateral from bregma, and -2.4 mm dorsoventral form the skull surface. The virus was injected using a Nanomite Pump (704507; Pump 11 Elite; Harvard Apparatus) at a rate of 0.2 μl/min and the needle was removed 5 minutes after the injection was complete in order to prevent backflow. Post-operation recovery from anesthesia occurred in a 37°C incubator until mice were awake and responsive. Buprenorphine was given to the mice as an analgesic (0.05 mg/kg, subcutaneous injection) one hour before surgery, as well as 6 and 12 hours after viral injection.

2.4 Tamoxifen Administration

Tamoxifen (TAM) was administered via intraperitoneal (IP) injection at a dosage of 160 mg/kg/day for 5days (dissolved in 10% EtOH and 90% sunflower oil) to 5-week-old Beclin1 nKO and control mice, similar to previously published work (Lagace et al., 2007). For all experimental time points (14, 30, and 60 days post injection of TAM) a minimum of 3 animals per genotype were analyzed.

2.5 Perfusion and Tissue Collection

Mice were anesthetized with euthanyl (90 mg/kg) and transcardially perfused with cold 1X phosphate buffer solution (PBS, pH 7.4) for 6 minutes and subsequently cold 4% paraformaldehyde in 1X PBS (pH 7.4) for 15 minutes at rate of 7 ml/minute. Brains were

removed and postfixed in 4% paraformaldehyde for 1 hour and then transferred to 30% sucrose in 1X PBS for cryoprotection. Brains were coronally sectioned into 30 μm slices with a freezing microtome (Leica SM 2000R) and stored in PBS with 0.1% sodium azide.

2.6 Antibodies and Immunohistochemistry

All primary and secondary antibodies used for immunohistochemistry (IHC) are listed in Table 2. Notably, a Green Fluorescent Protein (GFP) primary chicken antibody was used to detect both YFP immunoreactive (YFP+) cells in the Beclin1 nKO mice and GFP-Cre (GFP+) cells in the virally injected fBeclin1 mice.

Slide-mounted IHC was used to detect the total number of YFP+, DCX+, Ki67+ and AC3+ cells within the SGZ using previously published protocols (Lagace et al., 2007; Lagace et al., 2010). Briefly, every ninth section through the mouse hippocampus was mounted onto charged slides and allowed to dry overnight. Slides were then pre-treated with 0.1M citric acid (pH 6.0) at approximately 95°C for 15 minutes for antigen retrieval. For YFP and activated caspase 3 (AC3) staining additional antigen retrieval steps included incubation at room temperature (RT) in 0.1% trypsin for 10 minutes followed by 2N hydrochloric acid (HCl) for 30 minutes. To prevent non-specific binding, slides were incubated in 3% Normal Donkey Serum (NDS; 017-000-121; Jackson Immuno Research Laboratories Inc.) and 0.3% Triton X-100 in 1X tris-buffer saline (TBS) for 60 minutes. Sections were then incubated overnight in the primary antibody in 3% NDS in 0.3% Tween20 and 1X TBS. The following day, slides were incubated at RT in: 1) biotinylated attached secondary antibodies in 1.5% NDS in 1X TBS for 60 minutes; 2) 0.3% H_2O_2 in 1X TBS for 30 minutes to quench endogenous peroxidases; 3) Avidin-Biotin Complex Solution (ABC, PK-6100; Vector Laboratories) for 90 minutes; 4) metal

Table 2. List of Primary and Secondary Antibodies.

Primary Antibody	Company	Catalogue #	Concentration
Chicken-Anti-GFP	Aves	GFP-1020	1:5000
Living Colors Rabbit-Anti-DsRed Polyclonal Antibody	Clontech	632496	1:5000
Goat-Anti-DCX (C-18)	Santa Cruz	SC8066	1:1000
Rabbit-Anti-Ki67 Monoclonal Antibody	Medicorp	275R-14	1:100
Mouse-Anti-Glial Fibrillary Acidic Protein (GFAP)	Millipore	MAB3402	1:250
Mouse-Anti-NeuN Clone A60	Millipore	MAB377	1:500
Rabbit-Anti-Cleaved Caspase-3 (Asp175) (5A1E) Monoclonal Antibody	Cell Signalling Technology	9664S	1:250
Goat-Anti-Nestin	R&D Systems	AF2736	1:500
Secondary Antibody	**Company**	**Catalogue #**	**Concentration**
Biotin-SP-AffiniPure Donkey Anti-Chicken IgY (IgG)	Jackson Laboratories	703-065-155	1:200
Biotin-SP-AffiniPure Donkey Anti-Rabbit IgG	Jackson Laboratories	711-065-152	1:200
Biotin-SP-AffiniPure Donkey Anti-Goat IgG	Jackson Laboratories	705-065-147	1:200
Alexa Fluor 488 AffiniPure F(ab')2 Fragment Donkey Anti-Chicken IgY (IgG) (H+L)	Jackson Laboratories	703-546-155	1:500
Alexa Fluor 594 AffiniPure F(ab')2 Fragment Donkey Anti-Goat IgG (H+L)	Jackson Laboratories	705-586-147	1:500
Alexa Fluor 647 AffiniPure F(ab')2 Fragment Donkey Anti-Goat IgG (H+L)	Jackson Laboratories	705-606-147	1:500
Alexa Fluor 594 AffiniPure F(ab')2 Fragment Donkey Anti-Mouse IgG (H+L)	Jackson Laboratories	715-586-150	1:500
Alexa Fluor 647 AffiniPure F(ab')2 Fragment Donkey Anti-Mouse IgG (H+L)	Jackson Laboratories	715-606-150	1:500
Alexa Fluor 594 AffiniPure F(ab')2 Fragment Donkey Anti-Rabbit IgG (H+L)	Jackson Laboratories	711-586-152	1:500

enhanced 3,3'-Diaminobenzidine (DAB; 34065; Thermo Scientific, 1:10) for 10-30 minutes; and 5) fast red nuclear stain (H3403; Cedarlane) for counterstaining. Between all steps, with exception of after blocking with NDS, the slides were rinsed 3x with 1X TBS. Following staining, slides were dehydrated by consecutively immersing slides in 95% and 100% ethanol for 20 seconds, followed by CitriSolv clearing agent (22-143-975; Fisher) for 20 seconds, 1 minutes, and 5 minutes. Slides were cover-slipped with DPX mounting medium (mixture of Distyrene, Plasticizer, Xylene; 44581; Sigma).

All florescent IHC was completed using free-floating IHC methodology similar to those previously published (Lagace et al., 2007; Lagace et al., 2010). Briefly, sections were incubated in a carrier solution (1X PBS, 0.1% TritonX-100, 0.1% Tween20) on a shaker overnight with primary antibody at 4°C. The following day, the sections were incubated at RT in CY2, CY3, or CY5 flurophore attached secondary antibody for 1 hour in carrier solution, washed in 1X PBS and counterstained with 4',6-diamidino-2-phenylindole (DAPI, 11836170001; Roche, 1:10000). Following staining sections were slide mounted and cover-slipped with Immumount mounting media (2860060; Fisher Scientific).

2.7 Microscopy and Cellular Quantification

The number of immunoreactive cells in the SGZ of the dentate gyrus were manually quantified in every ninth coronal brain section using stereological methods as previously published (Lagace et al., 2007; Lagace et al., 2010). For the retroviral experiments, the number of GFP+, RFP+, and dual-labelled GFP+RFP+ cells were quantified in every ninth coronal section and multiplied by 9 to obtain an estimate of the total number of immunoreactive cells, or expressed as a ration of dual-labelled GFP+RFP+ cells over total RFP+ as previously published (Tashiro et al., 2006b). In the Beclin1 nKO mice, the

number of individual cells was quantified in every ninth half-coronal section and multiplied by 18 to estimate the total immunoreactive cell number in the SGZ.

All counts of DAB+ cells were performed at 40x magnification using an Olympus BX51 fluorescent microscope and recorded with a manual counter by a blinded experimenter. Quantification was further verified by an additional blinded experimenter that confirmed less than 10% variation in 2 independent counts.

For analysis of florescent immunoreactive cells, the SGZ was imaged at 40x (oil immersion) from Bregma matched (positions -2.06 to -2.30) coronal half-brain sections with a Zeiss LSM 510-META confocal microscope at emission wavelengths of 405, 488, 543, and 633. ZEN 2009 acquisition software (Zeiss) was used for 1 μm optical sectioning in the Z-plane. Both single- and co-labeled cells were quantified manually from images visualized through Fiji image processing software (ImageJ). The total population of YFP+ cells that co-labeled with another marker was calculated as the product of the absolute YFP counts and the proportion co-labeled per animal.

For analysis of spine density GFP and RFP co-labeled cells were imaged at 63x (oil immersion) with a Quorum Spinning-disk confocal microscope at emission wavelengths of 406, 490, and 561. MetaMorph automation and image acquisition software (Molecular Devices) was used to create a high resolution three dimensional representation of spines throughout the visible dendritic arbor using 0.5 μm Z-plane optical sectioning in combination with a tile-scan module. Images were subsequently stitched and flattened in MetaMorph and exported to NeuroStudio (CNIC, Ichan School of Medicine at Mount Sinai) to measure neurite length. Spines were manually quantified from a single neurite that spanned the hippocampal molecular layer (top of the granule cell layer to the

hippocampal fissure) per cell in Fiji image processing software (ImageJ). Spine density (spines/10 μm) was calculated as the quotient of the number of spines over neurite length multiplied by 10 (methods adapted from Zhao et al. (2006)).

2.8 Neural Stem Cell Culture

Beclin1 nKO mice were administered TAM and sacrificed two weeks post-treatment for neurosphere assay ((Babu et al., 2011). The SVZ tissue was dissected and incubated in a digestion media containing DMEM/F12 (11039-021; Invitrogen), 1.2 mM EDTA (E5134-1KG; Sigma), and 20 U/ml papain (LS003126, Worthington Biochemical) at 37°C for 30 min. Cells were titurated followed by centrifugation to obtain a cell pellet that was suspended in media containing DMEM/F12 and 10% Fetal Bovine Serum (FBS; SH3039603; Fisher) to inactivate papain. Cells were again titurated, centrifuged, then filtered and washed with DMEM/F12 to remove excess FBS. The resulting cell suspension was combined with growth media containing DMEM/F12, 1X B27 supplement (17504044; Invitrogen), 1X HyClone Penicillin-Streptomycin antibiotic solution (SV30010; Fisher), Heparin (H3149-25KU; Sigma), 200 ng/μl of Epidermal Growth Factor (EGF), and 100 ng/μl of Fibroblast Growth Factor (FGF). The cells were plated in a T75 or T25 flask at a clonal density of 10,000 cells/ml, and expanded for five days.

2.9 Flow Cytometry

Neurosphere cultures were collected and dissociated with tituration and incubation in TrypLE (12604-013; Invitrogen) at 37°C. Enzymatic activity was neutralized with media containing DMEM/F12 and 10% FBS and cells were washed with additional DMEM/F12 to remove excess FBS. Cells were then passed through 40 μm cell strainer (08-771-1,

Fisher), centrifuged, the supernatant was discarded and the cell pellet was resuspended in DMEM/F12 and the samples were kept on ice until sort. Cells were sorted using the University of Ottawa Cell Sorting Facility by Dr. Vera Tang. The sorting occurred using a MoFlo Astrios cell sorter (A66831; Beckman Coulter) using a 488 nm laser. Following collection the cells were centrifuged, flash frozen with liquid nitrogen, and stored at -80°C.

2.10 Western Blot

To perform a western blot analysis, cultured cells were collected and lysed in 8 mM urea with 10% sodium dodecyl sulfate (SDS). The lysed samples were mixed with an equal volume of laemmli loading buffer with 10% b-mercaptoethanol, boiled at 95°C, vortexed, and loaded onto a 12% acrylamide gel. The gel was immersed in 1X tris/glycine/SDS (TGS) running buffer and run at 110V for 1.5 hours for optimal band separation. Bands were transferred to a nitrocellulose membrane via a wet transfer in cold 1X Tris/Glycine transfer buffer containing 20% methanol for 1 hour at 110V.

The nitrocellulose member was cut into two for detection of Beclin1 (60 kDa) and HistoneH3 (18 kDa). The blots were incubated for 1 hour at RT in a blocking solution containing 5% non-fat dried milk in 1X TBS-T (0.1% Tween-20 in 1X TBS) followed by incubation in blocking solution containing either the primary antibody for Beclin1 (1:1000, SC11427, Santa Cruz) or HistoneH3 (1:1000, ab1791, Abcam) overnight at 4°C. The following day at RT the blots were washed with TBS-T and incubated for 1 hour in blocking solution containing corresponding horseradish peroxidase conjugated secondary antibodies (1:5000). After secondary incubation, the blots were washed in TBS-T incubated in ECL Pierce for 5 minutes to allow chemiluminescence detection. The blot

was imaged using a Fuji LAS-4000mini chemiluminescence imager and densitometry was performed using Fiji image processing software (ImageJ) to determine relative amounts of protein.

2.11 Statistical Analysis

All outcomes are reported as mean ± standard error of the mean (SEM) and were calculated and statistically analyzed using Prism 6.0 (GraphPad). Experiments with two groups were analyzed by a two-tailed student's t-test. Statistical analysis of three or more groups was performed using an ANOVA test, followed by a Bonferroni post hoc. Statistical significance was defined as $P < 0.05$. Notably, for the fBeclin1 retroviral analysis, any hemisphere with <90 RFP+ cells was excluded from analysis.

Results

3.1 Retroviral Mediated Removal of Beclin1 from Dividing NPCs Reduces Survival of Adult-Generated Neurons

To investigate whether Beclin1 regulates the survival and development of NPCs, a retroviral-mediated gene transfer strategy was employed to target Beclin1 removal in a small proportion of the proliferating NPC population. As previously published (Tashiro et al., 2006b), a dual-labeling retroviral system was implement in which two retroviruses, the CAG-GFP-Cre and a CAG-RFP, are stereotaxically injected in a 1:1 ratio into the dentate gyrus. As a result, dividing NPCs infected with CAG-GFP-Cre express GFP and have ablated Beclin1 expression in fBeclin1 mice, while dividing NPCs infected with CAG-RFP express RFP and have no alteration to Beclin1 expression. Therefore, infected cells that are either green (GFP+) or yellow (GFP+RFP+) have Beclin1 permanently removed fBeclin1 mice, while cells that are only red (RFP+) are WT for Beclin1 (Figure 4). This allows for comparison with two independent control groups: 1) GFP+ NPCs in WT littermates, and 2) RFP+ NPCs in both fBeclin1 mice and WT littermates. In addition, this model is advantageous as it targets only a small portion the dividing NPCs, limiting possible extrinsic effects when a large proportion of the NPC population is altered as in our Beclin1 nKO mice, thus allowing a better assessment of the cell-autonomous role of Beclin1 in NPC survival and maturation.

To determine whether Beclin1 is required for proliferating NPC survival over time, we quantified the number of GFP+ cells at 14, 30, and 60 days post injection (dpi) in fBeclin1 mice and WT controls (Figure 4B). There was a significant decrease in the number of GFP+ cells between fBeclin1 and WT mice. In addition, there was a trend for

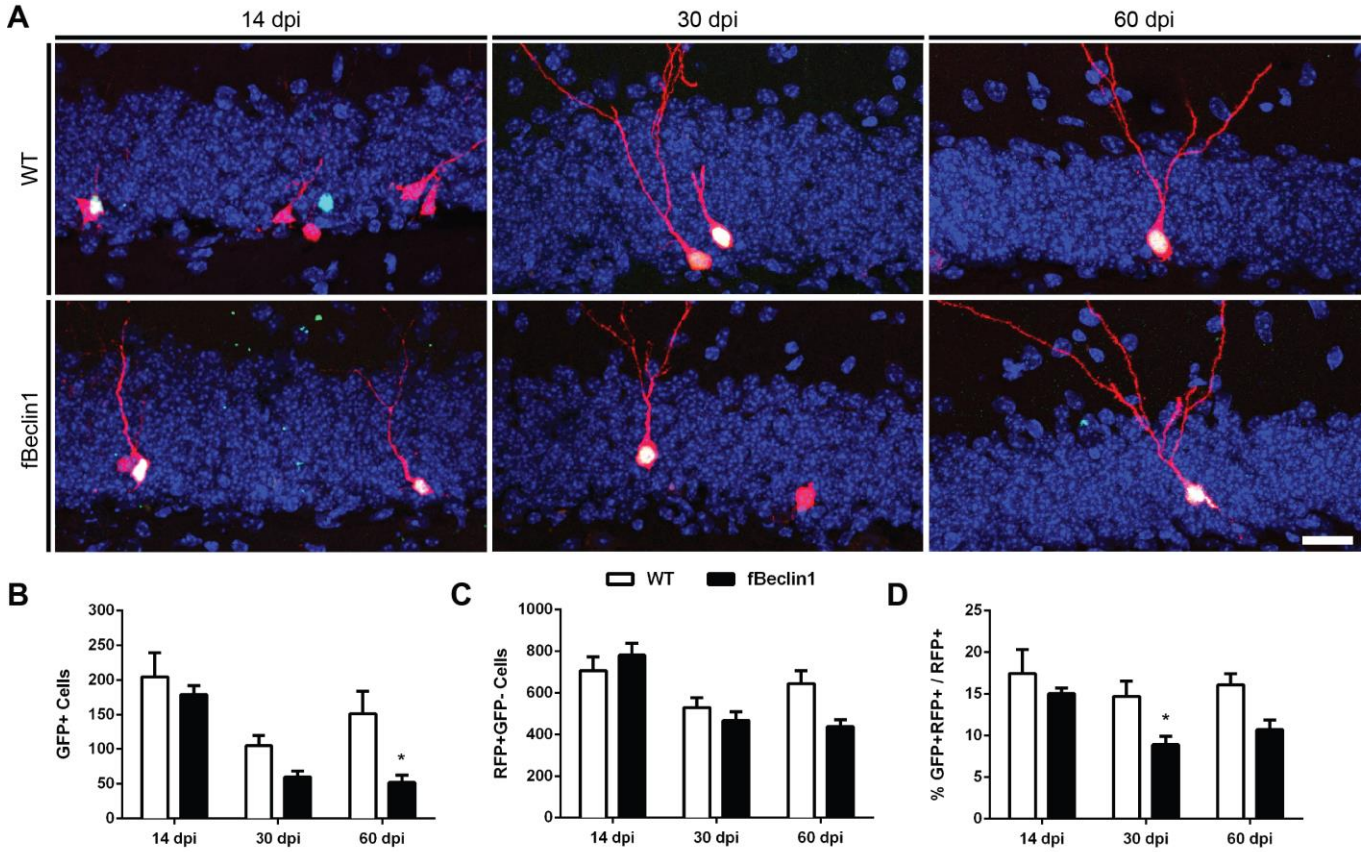

Figure 4. Retroviral-mediated removal of Beclin1 from proliferating NPCs reduces cell survival. **A)** Representative image of single labeled RFP (red), GFP (green), and double-labeled (yellow) cells at either 14, 30, or 60 dpi following injection of retroviruses (*CAG-GFP-Cre* and *CAG-RFP*) into the dentate gyrus of WT and fBeclin1 mice. Blue is DAPI. Scale bar is 20 μm. **B)** Quantification of GFP+ NPCs revealed a significant difference between fBeclin1 and WT mice ($F_{(1,65)} = 12.00$; $P = 0.0009$), a significant difference over time ($F_{(2,65)} = 20.45$; $P < 0.0001$), and no interaction between time and genotype. Posthoc analysis indicated a significant reduction at 60 dpi (*; $P < 0.05$). **C)** Quantification of RFP+GFP- cells revealed a significant difference over time ($F_{(2,65)} = 12.28$; $P < 0.0001$), and no difference in genotype or an interaction between time and genotype. **D)** Analysis of the survival of NPCs, measured as a ratio of double-labeled cell over total RFP+ cells, revealed a significant difference between fBeclin1 and WT mice ($F_{(1,34)} = 10.02$; $P = 0.0033$), a significant difference over time ($F_{(2,34)} = 4.26$; $P < 0.0223$), and no interaction between time and genotype. Posthoc analysis indicated a significant reduction at 30 dpi (*; $P < 0.05$). Error bars are SEM, posthoc analysis * $P < 0.05$, n = minimum of 90 RFP+ cells per injection, n = 4-10 animals per group.

a reduction in the number of GFP+ cells at 30 dpi in fBeclin1 mice, and a significant reduction at 60 dpi. This result did not occur from differences in viral infectivity or amount of cell death in WT and fBeclin1 mice since there was no there was no significant difference in the number of infected RFP+ cells between fBeclin1 and WT mice at all time points (Figure 4C). As expected, there was a significant reduction in GFP+ cells and RFP+ cells over time since the majority of NPCs undergo cell death during their development (Sierra et al., 2010).

To assess the survival of Beclin1-null NPCs, as previously reported (Tashiro et al., 2006a; Jagasia et al., 2009) we examined the ratio of the double-labeled GFP+RFP+ cells over the RFP+ control cells in both fBeclin1 and WT mice (Figure 4D). Similar to the GFP+ cell analysis, there was a significant decrease in NPC survival in fBeclin1 mice compared to WT controls. Furthermore, there was a significant reduction by posthoc analysis in the survival of Beclin1-null NPCs at 30 dpi, and a trend for a reduction at 60 dpi. Overall, these results demonstrate that viral-mediated removal of Beclin1 from dividing NPCs reduces survival beginning approximately one-month post Beclin1 ablation. Additionally, these results suggest that Beclin1 regulates survival of dividing NPCs in a cell-autonomous manner.

3.2 Retroviral Mediated Removal of Beclin1 from Dividing NPCs does not Alter the Fate of the NPC or Spine Development

To assess if Beclin1 has a cell-autonomous role in the development of the virally infected NPCs, fBeclin1 mice and WT controls were injected with the CAG-GFP-Cre retrovirus. In this experiment, the rapidly dividing NPCs were only labeled with the CAG-GFP-Cre virus in order to allow for co-labeling of GFP+ cells with two additional neurogenic

markers for phenotypic analysis (Figure 5A). Similar to our inducible model, we analyzed the proportion of GFP+ cells that co-labeled with DCX (Figure 5B), NeuN (Figure 5C), or both neuronal markers (Figure 5D) at 30 dpi. There was no difference in the proportion of Beclin1-null GFP+ cells in fBeclin1 mice that expressed DCX or NeuN, or both DCX and NeuN compared to Beclin1-expressing GFP+ cells in WT mice. This result demonstrates that retroviral-mediated removal of Beclin1 from dividing NPCs does not impede neuronal maturation one-month post ablation. Combined, these results suggest that Beclin1 is important in regulating the survival of dividing NPCs cell-autonomously in the absence of changing their fate.

Although there was no change in the fate of developing Beclin1-null NPCs, it is possible that alternative aspects of neuronal maturation may be impeded by a lack of autophagy or Beclin1. For instance, a critical step in development for the survival of immature neurons is the formation of new synaptic inputs and integration into the surrounding neuronal network (Christian et al., 2014). Interestingly, recent evidence demonstrated that ablation of autophagy resulted in spine pruning deficits (Tang et al., 2014). Thus, to assess whether Beclin1 removal from dividing NPCs altered spine development during neuronal maturation, we analyzed the spine density of GFP+RFP+ mature neurons in fBeclin1 and WT mice at 30 dpi (Figure 6). There was no difference in the spine density between fBeclin1 and WT mice one-month post Beclin1 removal from dividing NPCs. This result indicates that Beclin1 does not regulate spine formation cell-autonomously.

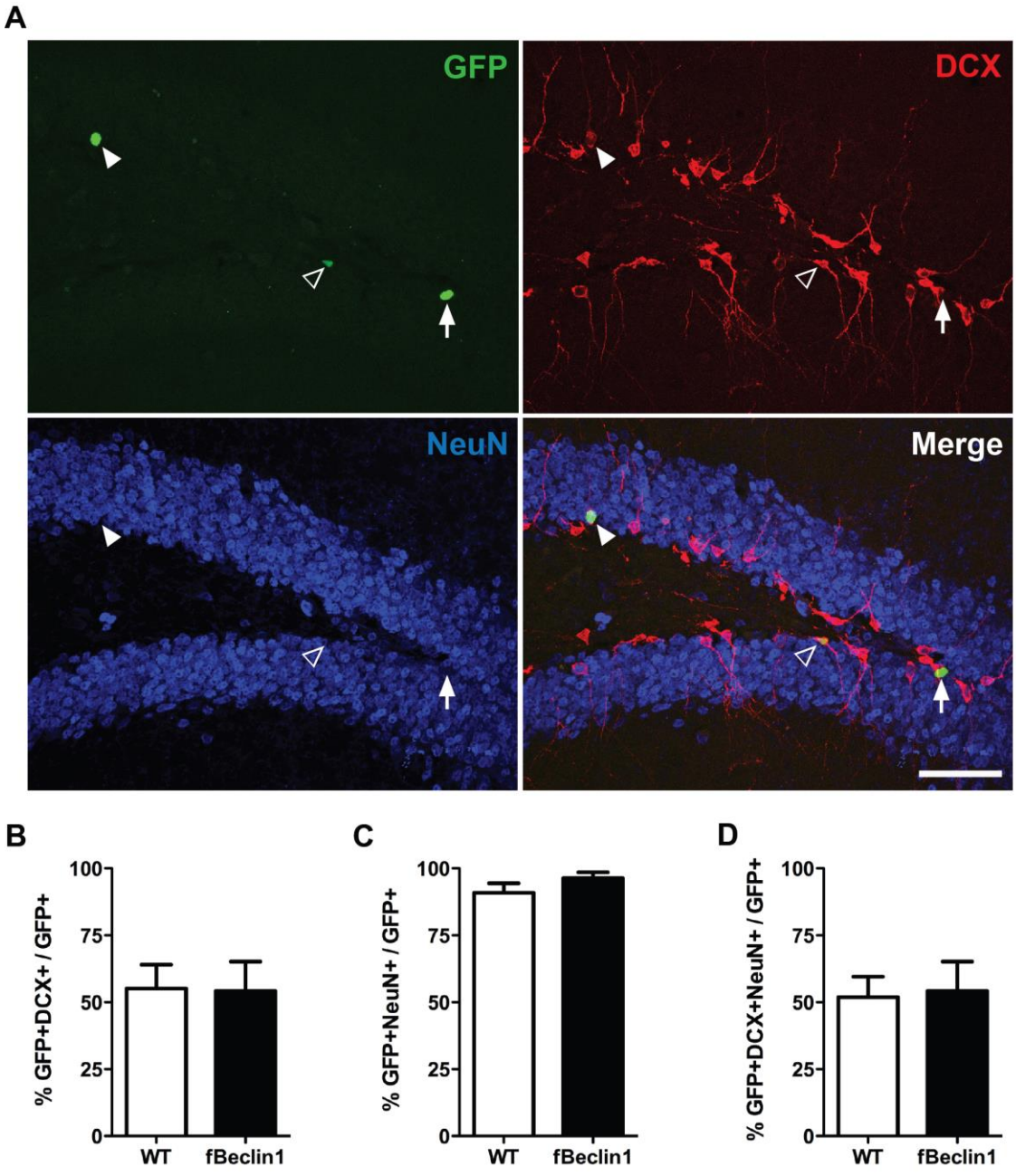

Figure 5. Retroviral-mediated removal of Beclin1 from proliferating NPCs does not alter neuronal fate. A) Representative image of GFP+ recombined cells that co-label with DCX (open arrowhead), NeuN (arrow), or both (closed arrowhead). Scale bar is 50 μm. The proportion of GFP+ recombined cells that co-labeled with **B)** DCX, **C)** NeuN, or **D)** both neuronal markers were similar in fBeclin1 animals compared to WT controls. Error bars are SEM, n = 20+ GFP+ cells per animal, n = 4 animals per genotype.

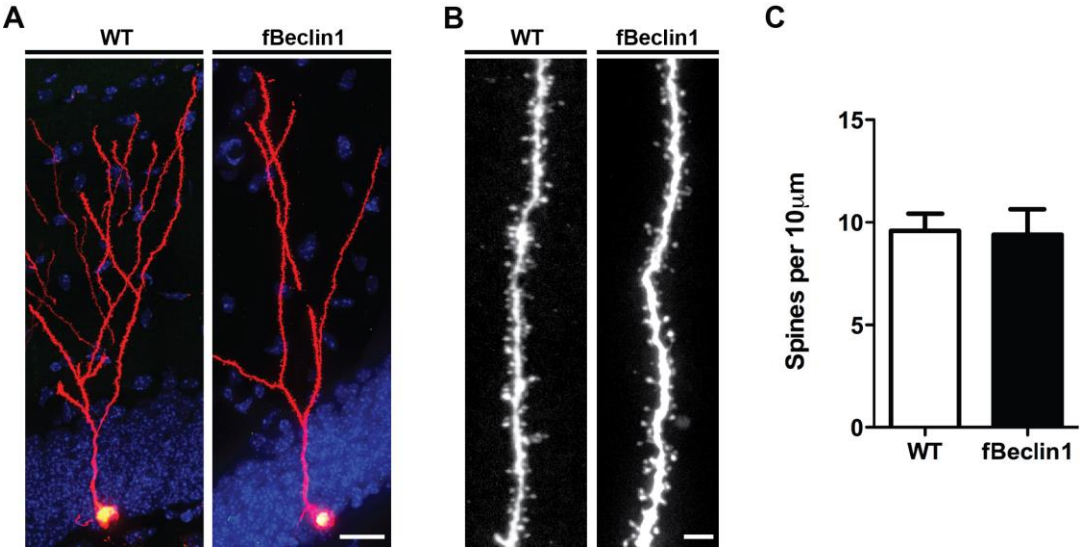

Figure 6. Removal of Beclin1 from dividing NPCs does not alter spine density at 30 days post injection. A) Representative image of double-labeled GFP+RFP+ cells at 30 dpi in WT and fBeclin1 mice. Blue is DAPI nuclear counterstain. Scale bar is 20 μm. **B)** Magnified image of spines from GFP+RFP+ cells at 30 dpi. Scale bar is 2 μm. **C)** Quantification of the number of spines per 10 μm reveals no difference in spine density between WT and fBeclin1 mice. Error bars are SEM, n = 2-4 cells per animal, n = 5 animals per genotype.

3.3 Generation of the Inducible Triple Transgenic Beclin1 Knockout Mouse

A current area under intense investigation in the adult neurogenesis field is determining the developmental stage(s) where cell fate decisions are made, and whether these decisions are made cell-autonomously or non-cell-autonomously (Ma et al., 2009; Bonaguidi et al., 2011; Ming and Song, 2011; Song et al., 2012). In our retroviral model, we demonstrated that Beclin1 removal from a small portion of the proliferating NPCs reduces the survival of adult-born neurons without altering fate. Considering retroviral-mediated gene transfer targets rapidly proliferating cells this model ablates Beclin1 from a small proportion of lineage-determined IPCs, without affecting multipotent RGLs (van Praag et al., 2002; Jagasia et al., 2009). Therefore, we asked whether Beclin1 removal from the RGL stem cell population and their progeny would impact the survival and development of NPCs in the adult SGZ.

In order to remove Beclin1 from RGLs and their progeny in the adult brain, we created a conditional Beclin1 knockout mouse model called the Beclin1 nKO mouse. The mouse is a triple transgenic that is generated using an inducible Nestin-CreER^{T2} (Imayoshi et al., 2006), a R26R-eYFP reporter (Srinivas et al., 2001), and a fBeclin1 transgene (McKnight et al., 2014) (Figure 7A). The Nestin-CreER^{T2} transgene is composed of a 5.8 kb fragment of the promoter region and a 1.8 kb fragment of the second intron of the nestin gene, which drives CreER^{T2} expression. Nestin is a class VI intermediate filament protein expressed in numerous cells in the brain, including adult NPCs of the neurogenic niche where it's expression has been linked to neuronal fate (Lendahl et al., 1990; Lagace et al., 2007; Hendrickson et al., 2011). Therefore, the inducible Nestin-CreER^{T2} transgene allows for genetic recombination in nestin-expressing cells under the temporal

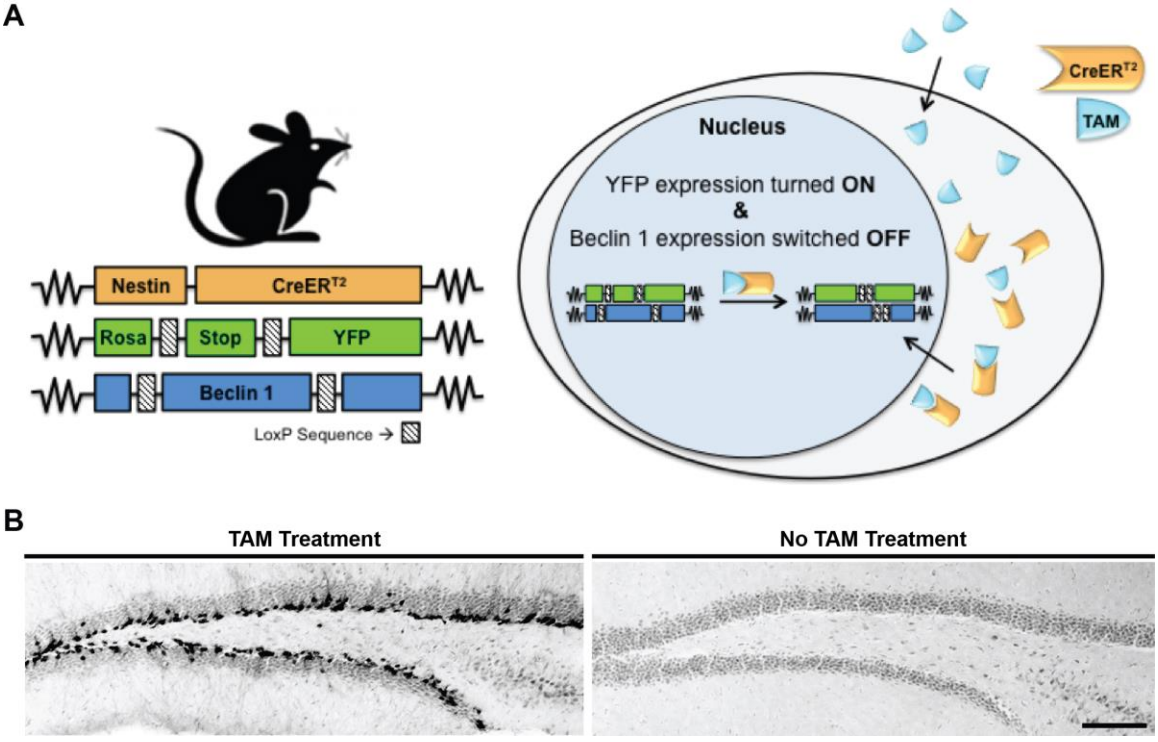

Figure 7. Creation of inducible Beclin1 nKO transgenic mouse model. A) The Nestin-CreER^{T2} contains 5.8kb of the nestin promoter and 1.8kb of the second intron of the nestin gene. The Rosa R26R-eYFP reporter mouse has a STOP codon between two loxP sites. The fBeclin1 gene has exon 2 flanked by loxP sites. TAM causes translocation of CreER^{T2} into nucleus to induce genetic recombination. **B)** Representative images of genetic recombination with and without TAM administration. Genetic recombination and expression of YFP only occurs with TAM treatment. Scale bar is 100 μm.

control of TAM administration. The advantage of this particular Nestin-CreER^{T2} is the promoter sequence restricts CreER^{T2} expression to nestin-expressing cells in the neurogenic niche. Furthermore, it is efficient as it allows for genetic recombination in approximately 65% of the nestin-expressing cell population in the SGZ (Imayoshi et al., 2008).

Floxed Beclin1 mice were crossed with the Nestin-CreER^{T2} transgenic mouse line to create a novel inducible Nestin-CreER^{T2} x fBeclin1 transgenic mouse model. In order to visualize which NPCs underwent CreER^{T2}-mediated genetic recombination, this double transgenic mouse was crossed with an R26R-eYFP reporter line that has a STOP codon flanked by loxP sites (Srinivas et al., 2001). The final cross resulted in a triple transgenic mouse line that was heterozygous for Nestin-CreER^{T2}, heterozygous for R26R-eYFP, and homozygous positive for fBeclin1 or WT Beclin1 (Beclin1 nKO or WT respectively). Administration of the estrogen ligand TAM to the Beclin1 nKO mice allows TAM to bind the estrogen receptor of CreER^{T2}, permitting its translocation into the nucleus where the Cre recombinase enzyme excises DNA segments flanked by loxP recognition sites. Therefore in Beclin1 nKO mice, Cre excises the second exon of fBeclin1 and the STOP codon of R26R-eYFP, simultaneously ablating Beclin1 expression and initiating the production of YFP+ Beclin1-null NPCs (Figure 7A).

Genetic recombination was first shown to be dependent on TAM. As expected, recombination and YFP expression was induced following TAM administration, and did not occur in non-TAM treated animals (Figure 7B). To verify that Beclin1 expression was ablated in YFP+ Beclin1-null NPCs, NPCs were isolated from Beclin1 nKO and WT controls 10 days following TAM treatment and expanded in culture as primary

neurospheres. After 5 days of expansion, neurospheres were FACS sorted to isolate YFP+ cells (Figure 8C,D). A total of 74,000 YFP+ cells were collected from WT neurospheres, representing the expanded recombined stem- and progenitor-like cell population. In contrast, just 29,300 YFP+ cells were isolated from the Beclin1 nKO neurospheres. As expected, a western blot for Beclin1 expression demonstrated a reduction in Beclin1 protein levels in YFP+ NPCs from Beclin1 nKO mice compared to an equal number of YFP+ NPCs from WT control mice (Figure 8A,B).

3.4 Removal of Beclin1 Reduces the Total Population of Nestin-Expressing NPCs and their Progeny

To assess the impact of Beclin1 removal on the survival of nestin-expressing NPCs and their progeny over time, the total population of recombined YFP+ NPCs in Beclin1 nKO and WT controls was quantified in the SGZ at 14, 30, and 60 dpi (Figure 9). In agreement with previous studies using the Nestin-CreER^{T2} mouse models (Lagace et al., 2007; Imayoshi et al., 2008), there was slight increase in the population of YFP+ cells in the WT mice from 14 to 30 dpi, followed by a plateau in the population from 30 to 60 dpi. This was expected since this model allows for recombination in the nestin-expressing NPCs and their progeny, which expand the YFP+ cell population over time until plateau is reached. In contrast, in the Beclin1 nKO mice there was a significant reduction in the YFP+ cell population from 14 to 30 dpi, which was maintained at 60 dpi. Therefore, at 14 dpi, there was no difference in the number YFP+ NPCs in the Beclin1 nKO mice compared to WT controls. This was in contrast to 30 and 60 dpi, where there was an approximate 2-fold reduction in YFP+ cells in the Beclin1 nKO mice compared to the WT mice.

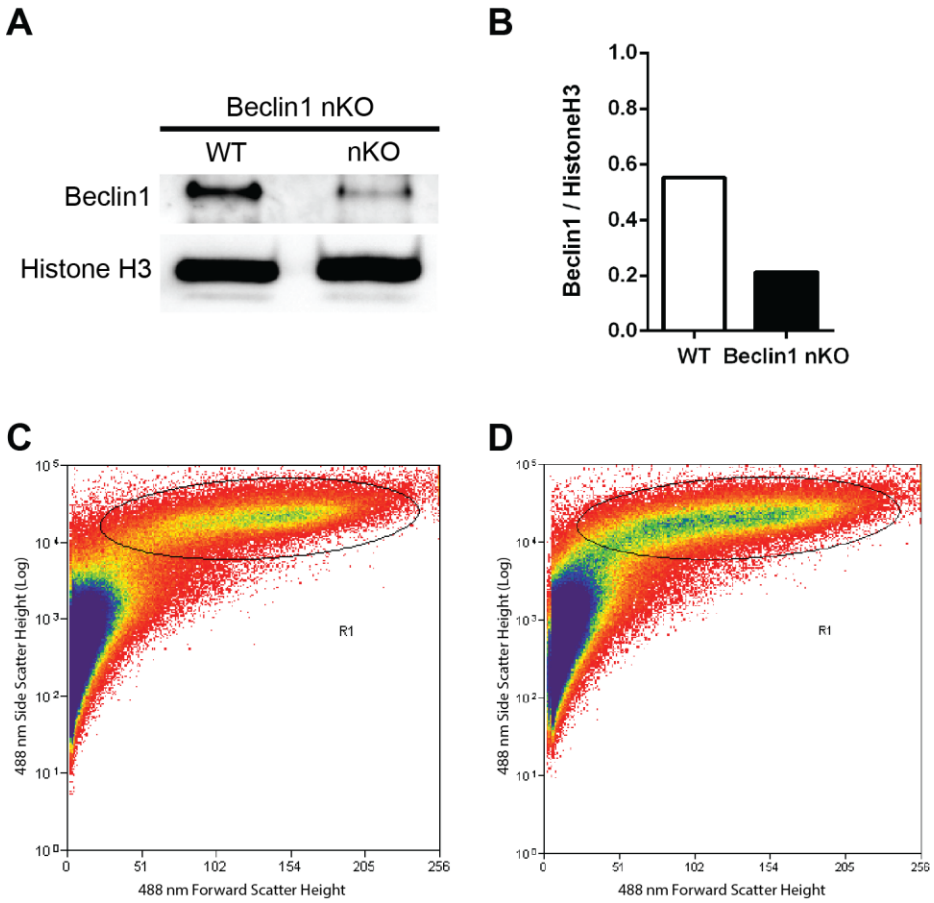

Figure 8. Beclin1 nKO neurospheres have a reduced amount of Beclin1 protein. **A)** Comparison of bands probed for Beclin1 and the loading control HistoneH3 in Beclin1 nKO and WT animals. **B)** Densitrometry reveals a reduction in the amount of Beclin1 protein in Beclin1 nKO mice, expressed a ratio of Beclin1 to HistoneH3. Graphic representation of the FACS sort for the **C)** WT and **D)** Beclin1 nKO neurospheres. R1 is the area of interest designating the live cell population that was sorted. Cells pooled from n=2 mice per genotype.

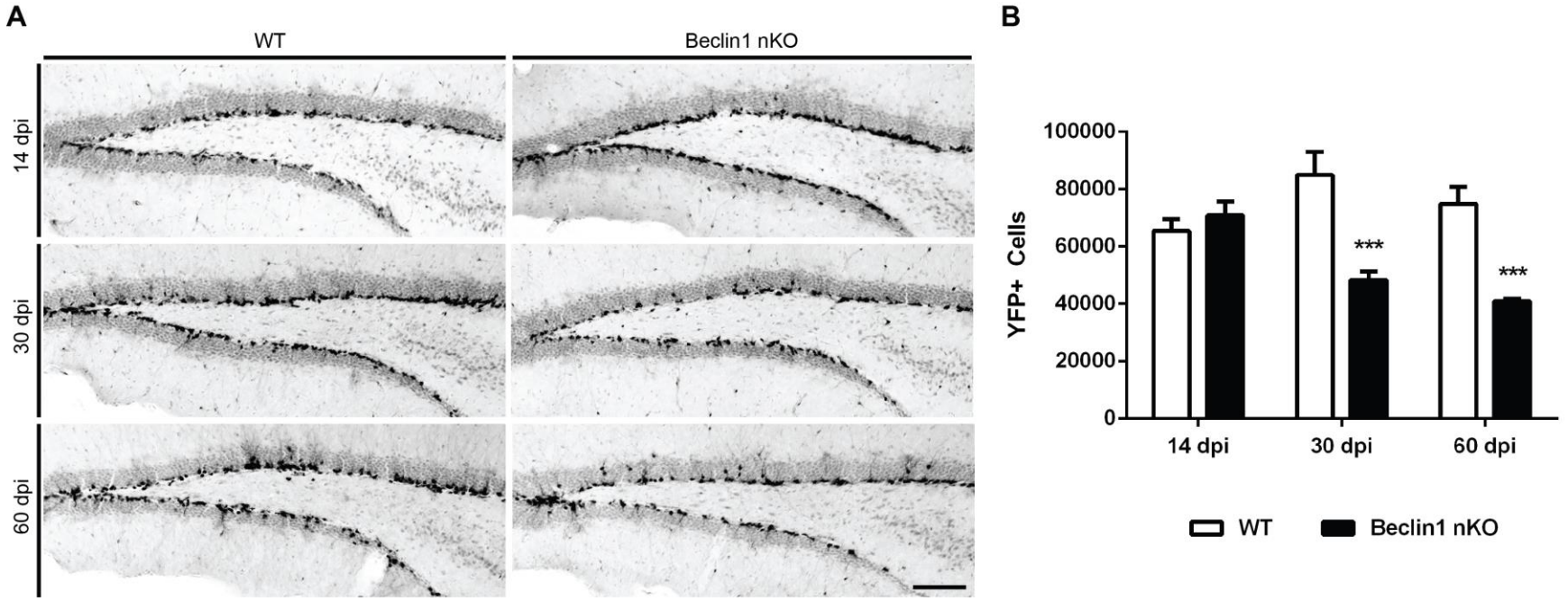

Figure 9. Beclin1 nKO mice have a significant reduction in the number of recombined YFP+ NPCs over time. A) Representative image of YFP+ recombined cells in both Beclin1 nKO and WT control mice at 14, 30, and 60 dpi. Scale bar is 100 μm. **B)** Quantification of YFP+ cells revealed a significant difference between Beclin1 nKO and WT controls ($F_{(1,21)}$ = 29.39; P < 0.0001), and a significant interaction between time and genotype ($F_{(2,21)}$ = 12.97; P = 0.0002). Posthoc analysis indicated significantly less Beclin1-null YFP+ cells at 30 and 60 dpi (***; P < 0.001). Error bars are SEM, n = 3-6 per group.

To determine if this reduction was coincident with an increase in cell death in the Beclin1 nKO mice, we quantified the number of cells that expressed the apoptotic marker AC3 (Figure 10). There was no difference in the number of AC3+ cells between Beclin1 nKO mice at WT controls, suggesting that the reduction in the YFP+ cell population observed in Beclin1 nKO was not due to cell death.

3.5 Removal of Beclin1 Reduces Adult Hippocampal Neurogenesis

The absence of an increase in AC3+ apoptotic cells coincident with the reduction in YFP+ NPCs prompted investigation into whether Beclin1 removal could alter NPC maturation in the SGZ, and at what stage during NPC development Beclin1 is required. This type of population analysis is possible with inducible Nestin-CreER^{T2} mouse models as it allows for genetic recombination in nestin-expressing NPCs and their progeny, which over time results in a developmentally heterogeneous YFP+ population (Lagace et al., 2007; Imayoshi et al., 2008). To ask whether the reduction in YFP+ cells over time translated to a reduction in the number of adult-born neurons, we quantified the proportion and total population of YFP+ cells that co-labeled with the mature neuronal marker NeuN at 30 dpi (Figure 11).

As predicted, there was a reduction in the proportion of YFP+ mature neurons that expressed NeuN, and YFP+ maturing neurons that expressed both DCX and NeuN. In addition, there was a 3-fold reduction in the total population of YFP+ NeuN+ mature neurons and in the total population of YFP+ DCX+ NeuN+ maturing neurons. These results suggest that removal of Beclin1 reduces the production of adult-born neurons.

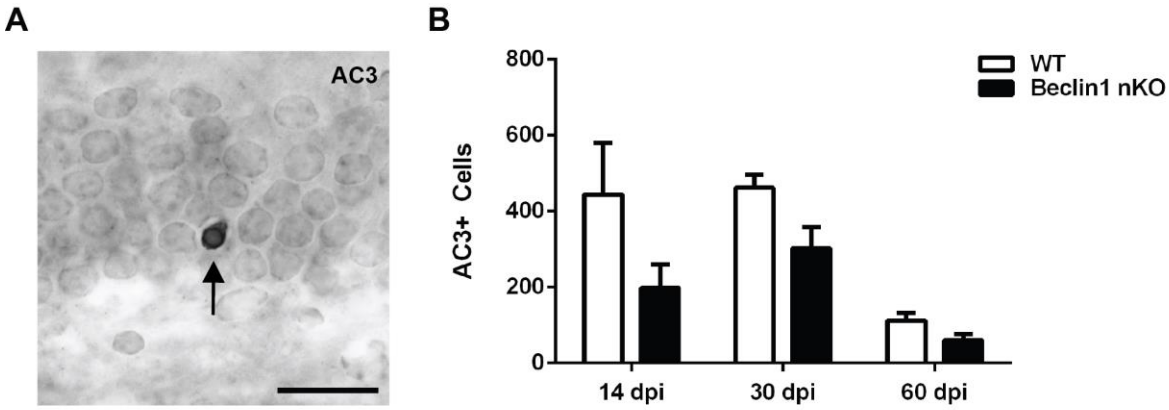

Figure 10. Beclin1 ablation does not increase apoptotic cell death marked by expression of activated-caspase 3 (AC3). A) Representative image of an AC3+ cell in Beclin1 nKO and WT mice at 14, 30, and 60 dpi. Scale bar is 50 μm. **B)** Quantification of the absolute population of AC3 expressing cells demonstrated a similar amount of apoptotic cell death between Beclin1 nKO and WT mice at 14, 30, and 60 dpi. Error bars are SEM, n = 3-6 per group.

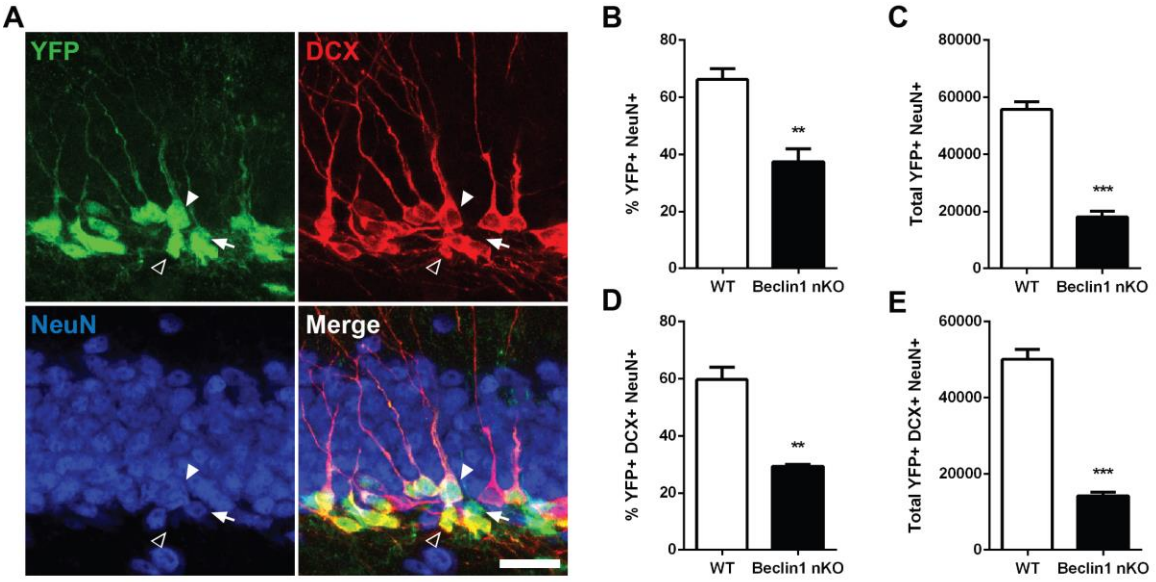

Figure 11. Beclin1 nKO mice have a reduction in YFP+ mature neurons at 30 dpi. A) Representative image of recombined YFP+ cells that express DCX (open arrowhead), NeuN (arrow), or both neuronal markers (arrowhead). Scale bar is 20 μm. There was a reduction in the **B)** proportion and **C)** the total population of mature YFP+ cells that co-labelled with NeuN in Beclin1 nKO mice at 30 dpi. There was a similar reduction in **D)** the proportion and **E)** the total population of maturing YFP+ cells that co-labeled with NeuN and DCX in Beclin1 nKO mice at 30 dpi. Error bars are SEM, n = 40+ YFP+ cells, n = 3 animals per group, t-test ** $p < 0.01$, *** $p < 0.001$.

The reduction in YFP+ adult-born neurons at 30 dpi led us to investigate the effect of Beclin1 removal on the population of immature neurons. We quantified the proportion and total population of YFP+ cells that co-labeled with the immature neuronal marker DCX (Figure 12). At 14 dpi, there was no difference in the proportion and total population of YFP+ cells that expressed DCX in Beclin1 nKO mice and WT controls. However, at 30 dpi, there was an approximate 2-fold reduction in the proportion and 3-fold reduction in the total population of YFP+ DCX+ cells.

To determine if the reduction of recombined immature neurons following Beclin1 would translate to a reduction in the absolute population of immature neurons, we quantified the number of DCX+ immature neurons in the adult SGZ in WT and Beclin1 nKO mice (Figure 13). Expectedly, we observed a similar reduction in the absolute population of DCX+ immature neurons over time, with a significant 2-fold reduction at 30 dpi that was maintained at 60 dpi. Combined, these results suggest that removal of Beclin1 from nestin-expressing NPCs reduces adult hippocampal neurogenesis.

3.6 Beclin1 Ablation Reduces the Population of Proliferating NPCs

The reduction in adult neurogenesis in the Beclin1 nKO mice prompted us to further investigate if this occurred due to an upstream reduction in number of proliferating NPCs since autophagy is suggested to regulate proliferation in the context of embryonic neurogenesis (Fimia et al., 2007; Vazquez et al., 2012; Wang et al., 2013; Lv et al., 2014). We first investigated the proliferative population of NPCs by assessing the proportion and total population of YFP+ cells that co-labeled with the proliferative cell cycle marker Ki67 (Figure 14). Although multiple developmental subpopulations can undergo proliferation in the SGZ, the most proliferative are intermediate precursor cells

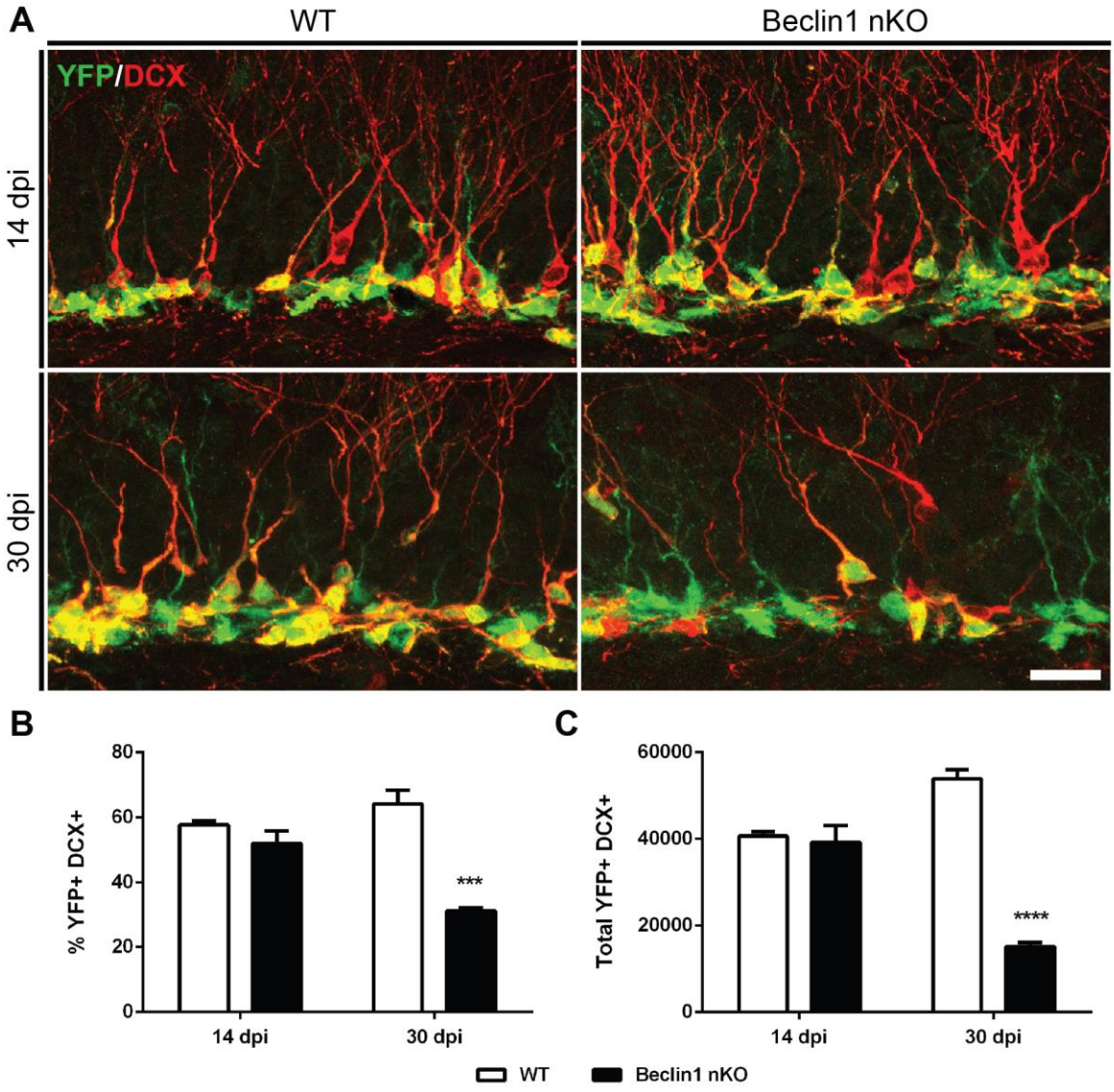

Figure 12. Beclin1 nKO mice have a reduction in YFP+ immature neurons over time. **A)** Representative confocal image of dual-labelled YFP+ (green) and DCX+ (red) cells at 14 and 30 dpi in Beclin1 nKO and WT mice. Scale bar is 20 μm. **B)** Quantification of the proportion of YFP+ cells that co-labeled with the immature neuronal marker DCX revealed a significant difference between Beclin1 nKO and WT controls ($F_{(1,8)}$ = 41.61; P = 0.0002), a significant difference over time ($F_{(1,8)}$ = 5.74; P = 0.0435), and a significant interaction between time and genotype ($F_{(1,8)}$ = 20.69; P = 0.0019). Posthoc analysis indicated a significant reduction at 30 dpi (***; P < 0.001). **C)** Quantification of the total population of YFP+ DCX+ revealed a significant difference between Beclin1 nKO and WT controls ($F_{(1,8)}$ = 73.59; P < 0.0001), a significant difference over time ($F_{(1,8)}$ = 5.49; P = 0.0472), and a significant interaction between time and genotype ($F_{(1,8)}$ = 63.23; P < 0.0001). Posthoc analysis indicated a significant reduction at 30 dpi (****; P < 0.0001). Error bars are SEM, n = 40+ YFP+ cells, n = 3 animals per group.

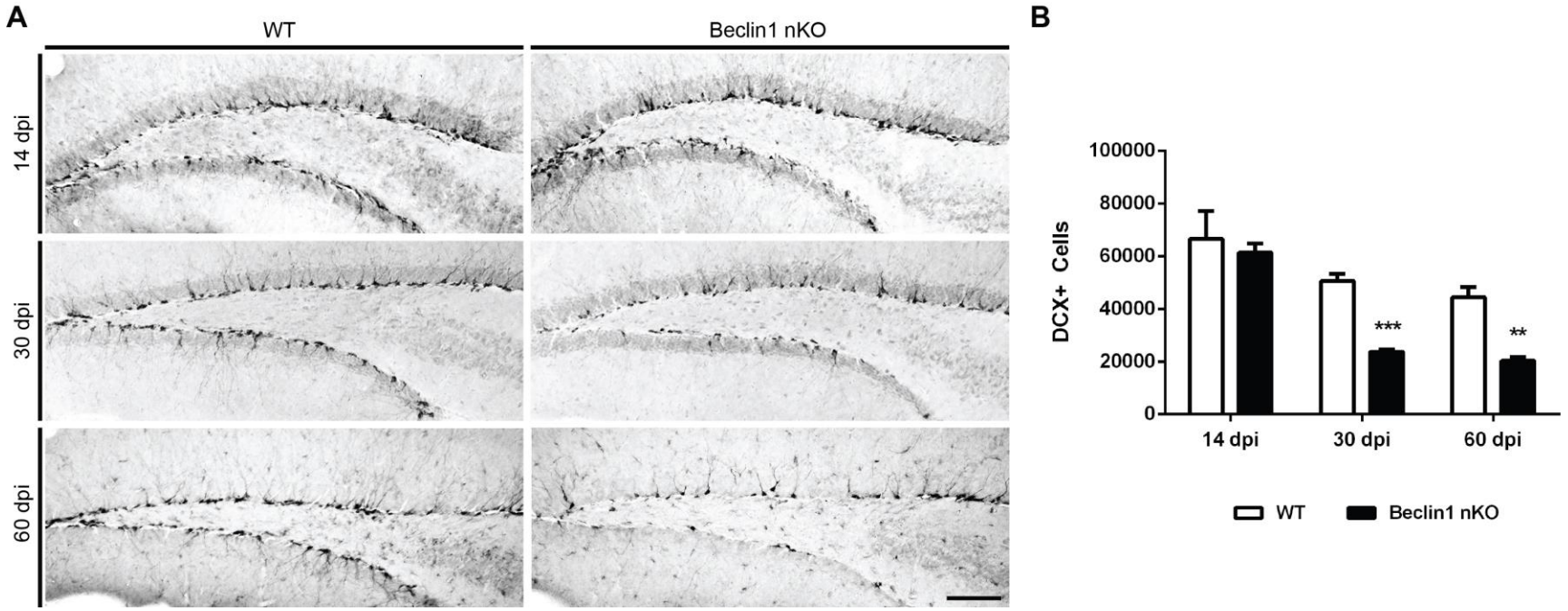

Figure 13. Beclin1 nKO mice have a reduction in the absolute population of immature neurons over time. A) Representative image of DCX+ immature neurons in both Beclin1 nKO and WT control mice at 14, 30, and 60 dpi. Scale bar is 100 μm. **B)** Quantification of the absolute population of DCX+ immature neurons revealed a significant difference between Beclin1 nKO and WT controls ($F_{(1,16)} = 29.47$; $P < 0.0001$), a significant difference over time ($F_{(2,16)} = 30.21$; $P < 0.0001$), and a significant interaction between time and genotype ($F_{(2,16)} = 3.70$; $P = 0.0479$). Posthoc analysis revealed significantly less DCX+ immature neurons at 30 and 60 dpi (**; $P < 0.01$, ***; $P < 0.001$). Error bars are SEM, n = 3-4 per group.

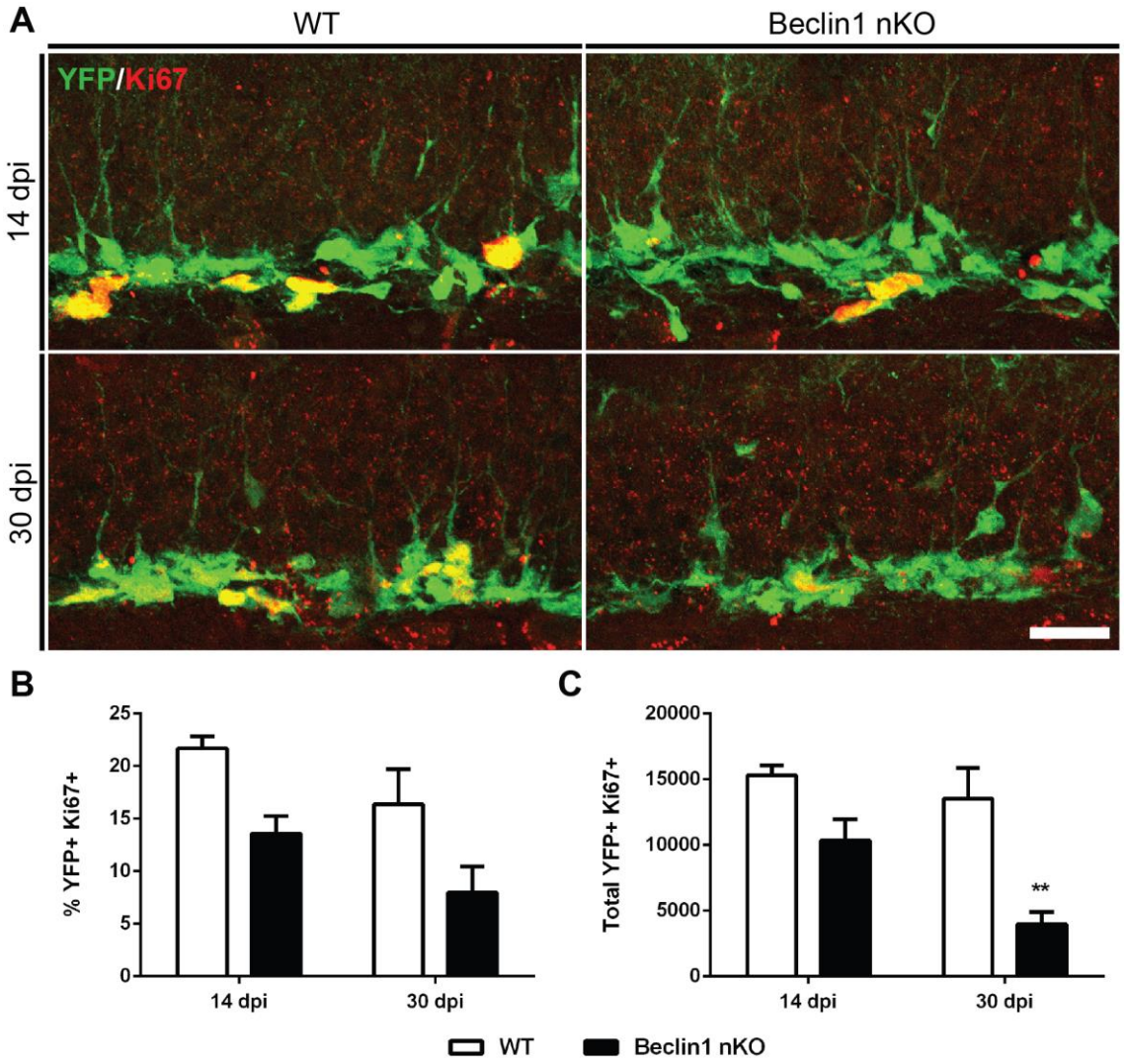

Figure 14. Beclin1 nKO mice have a reduction in the total population of YFP+ proliferating cells over time. A) Representative confocal image of dual-labelled YFP+ (green) and Ki67+ (red) cells at 14 and 30 dpi in Beclin1 nKO and WT mice. Scale bar is 20 μm. **B)** Quantification of the proportion of YFP+ cells that co-labeled with the proliferative marker Ki67 revealed a significant difference between Beclin1 nKO and WT controls ($F_{(1,8)} = 12.08$; $P = 0.0084$), a trend for a difference over time ($F_{(1,8)} = 4.22$; $P = 0.0741$), and no interaction between time and genotype. There is a trend towards a reduction in the proportion of YFP+ Ki67+ cells in Beclin1 nKO mice at both 14 and 30 dpi. **C)** Quantification of the total population of YFP+ Ki67+ cells revealed a significant difference between Beclin1 nKO and WT controls ($F_{(1,8)} = 20.46$; $P = 0.0019$), a trend for a difference over time ($F_{(1,8)} = 5.05$; $P = 0.0548$), and no interaction between time and genotype. Posthoc analysis indicated a significant reduction at 30 dpi (**; $P < 0.01$). Error bars are SEM, n = 400+ YFP+ cells, n = 3 animals per group.

(IPCs; type-2a, type2b, and type-3) or secondary transient amplifying cells, thus allowing cell cycle markers including Ki67 to label this subpopulation with a high degree specificity (Kronenberg et al., 2003; Kempermann et al., 2004). At both 14 and 30 dpi, there was a non-significant trend for a reduction in the proportion of YFP+ cells that co-labeled with Ki67 in Beclin1 nKO mice compared to WT controls (Figure 14B,C). Moreover, at 14 dpi there was a trend for a reduction, and at 30 dpi a significant reduction in the total population of YFP+ Ki67+ cells. This suggests the Beclin1 removal decreases the proliferating YFP+ IPC population in the adult SGZ.

The IPCs are divided into three subpopulations that have differential DCX expression, with the type-2a not expressing DCX and both the type-2b and type-3 expressing DCX (Kronenberg et al., 2003; Kempermann et al., 2004). To assess whether Beclin1 removal altered the IPC subpopulations, we analyzed the proportion and total population of YFP+ Ki67+ cells that were positive or negative for DCX expression (Figure 15). We found that there was a significant reduction in the proportion of YFP+ Ki67+ cells that co-labeled with DCX, as well as in the population of YFP+ Ki67+ cells that were negative for DCX at 14 dpi (Figure 15B,D). Moreover there was a significant reduction, and a trend for a reduction in the total population of YFP+ Ki67+ DCX+, and YFP+ Ki67+ DCX- cells respectively (Figure 15C,E). These results indicate that removal of Beclin1 reduces the proliferating NPC population irrespective of DCX expression, and thus irrespective of IPC subpopulation.

To ask whether the reduction in YFP+ proliferating cells at 14 and 30 dpi would translate to a decrease in the absolute population of proliferating cells, we quantified the total number of Ki67+ cells in the SGZ irrespective of YFP expression and developmental

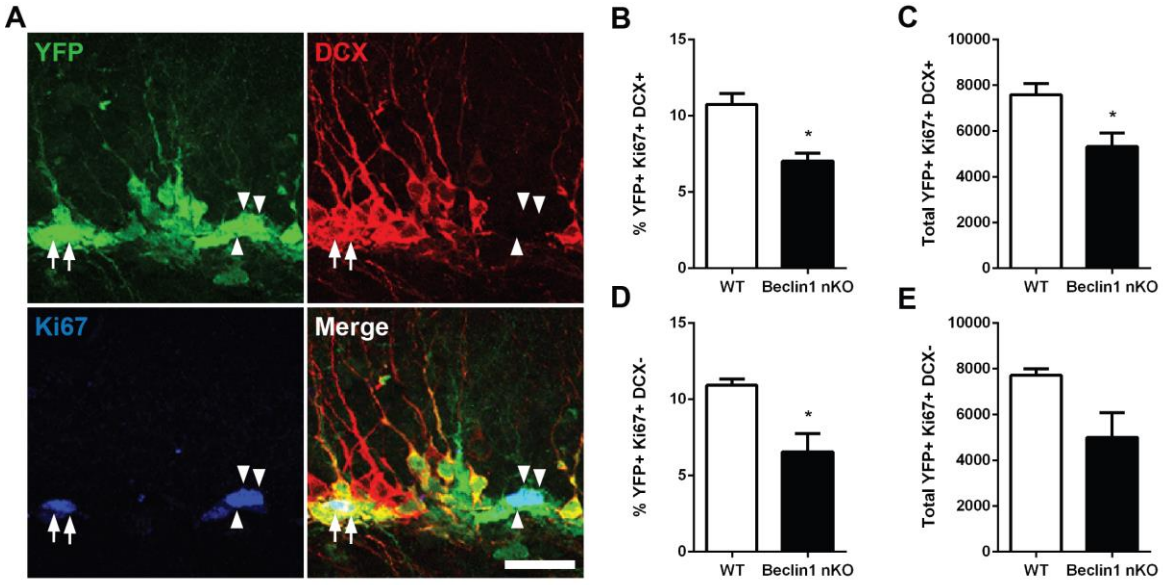

Figure 15. Beclin1 nKO mice have a reduction in the proportion of YFP+ proliferating NPCs at 14 dpi, irrespective of DCX expression. A) Representative image of recombined YFP+ cells that express Ki67 (arrowhead), or both Ki67 and DCX (arrow). Scale bar is 20 μm. There was a reduction in **B)** the proportion and **C)** the total population of proliferating YFP+ cells that co-labeled with Ki67 and DCX in Beclin1 nKO mice at 14 dpi. There was a similar reduction in **D)** the proportion and a trend for a reduction in **E)** the total population of proliferating YFP+ cells that co-labeled with Ki67 but not DCX in Beclin1 nKO mice at 14 dpi. Error bars are SEM, n = 500+ YFP+ cells, n = 3 animals per group, t-test * $p < 0.05$.

stage (Figure 16). We found a decrease in the absolute population of proliferating cells overtime, with an approximate 2-fold reduction in Ki67+ cells at 30 dpi, that was maintained at 60 dpi. As expected, since the rate of IPC proliferation decreases with age (Kuhn et al., 1996), we saw a decline in the absolute proliferating population over time in the WT mice that was exaggerated in the Beclin1 nKO mice. These results suggest a role of Beclin1 in regulating the proliferating NPCs in the adult SGZ.

3.7 Beclin1 Ablation Increases the Proportion of Radial Glia-like Stem Cells

Since Beclin1 removal resulted in a reduction in the proportion of YFP+ proliferating NPCs, immature neurons, and mature neurons at 30 dpi, we predicted this may be accompanied by a decrease in the proportion of RGL stem cells. To investigate the effect of Beclin1 removal on the RGL stem cell pool, we examined the proportion and total population YFP+ NPCs that co-labeled with Nestin and GFAP and extend a radial process through the granule cell layer (Figure 17). Although there is debate regarding which NPCs constitute the population of multipotent self-renewing stem cells in the SGZ, recent reports have identified Nestin and GFAP expressing radial glia-like cells as the likely *bona fide* stem cell (Lagace et al., 2007; Bonaguidi et al., 2011; Encinas et al., 2011; Song et al., 2012). Surprisingly, over time there was a significant increase in the proportion of RGLs in Beclin1 nKO mice, without an increase in the total population (Figure 6B,C). At 14 dpi there was neither an increase in the proportion or total population of RGLs however, at 30 dpi there was a significant increase in just the proportion of RGLs. This result indicates that Beclin1 removal increases the proportion of YFP+ RGL stem cells over time.

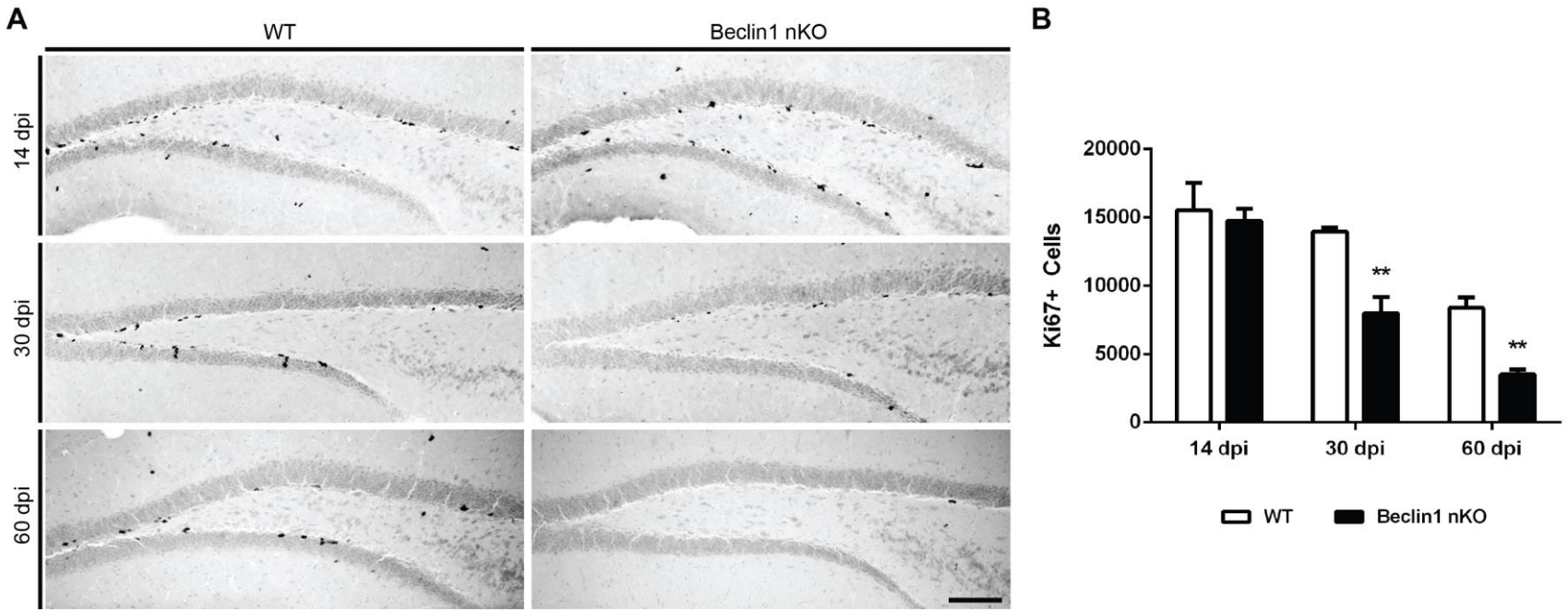

Figure 16. Beclin1 nKO mice have a reduction in the absolute population of proliferating cells at 30 dpi. A) Representative image of Ki67+ proliferating cells in both Beclin1 nKO and WT control mice at 14 and 30. Scale bar is 100 μm. **B)** Quantification of the absolute population of proliferating Ki67+ cells revealed a significant difference between Beclin1 nKO and WT controls ($F_{(1,14)}$ = 22.07; P < 0.0003), a significant difference over time ($F_{(2,14)}$ = 44.03; P < 0.0001), and a trend for an interaction between time and genotype ($F_{(2,14)}$ = 3.40; P = 0.0626). Posthoc analysis revealed significantly less Beclin1-null YFP+ cells at 30 and 60 dpi (**; P < 0.01). Error bars are SEM, n = 3-5 animals per group.

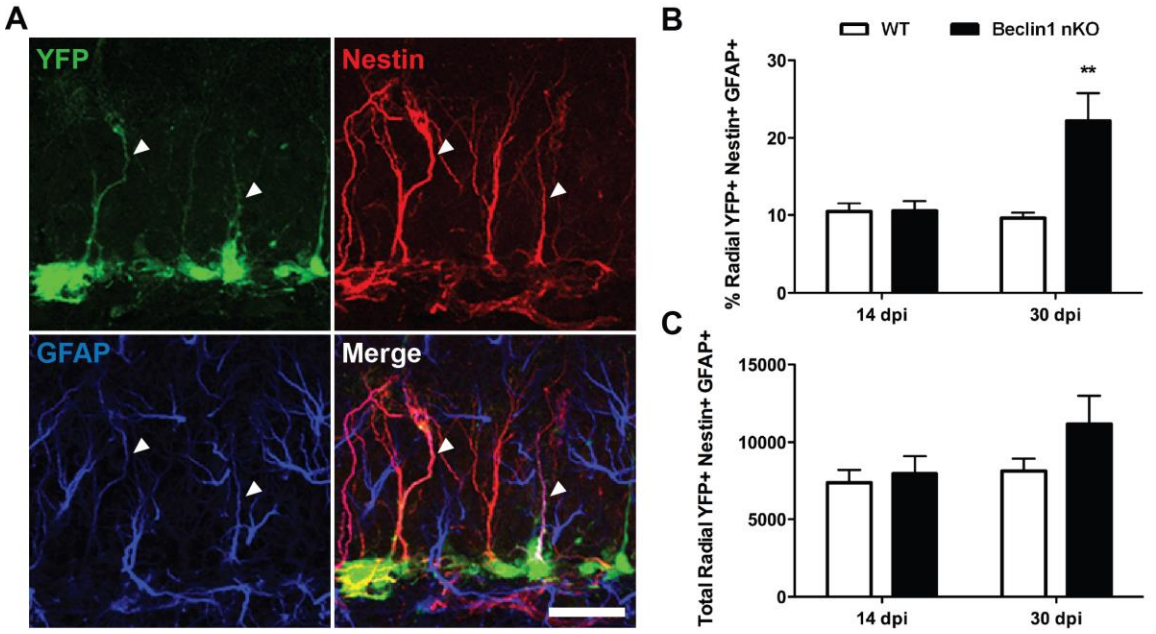

Figure 17. Beclin1 nKO mice have an increase in the proportion of YFP+ RGL stem cells at 30 dpi. **A)** Representative image of recombined a YFP+ radial glia stem-like NPCs that expresses Nestin and GFAP. Scale bar is 20 μm. **B)** Quantification of the proportion of YFP+ radial glia-like cells that co-labeled with Nestin and GFAP revealed a significant difference between Beclin1 nKO and WT controls ($F_{(1,8)}$ = 9.83; P = 0.0139), a significant difference over time ($F_{(1,8)}$ = 7.13; P = 0.0283), and a significant interaction between time and genotype ($F_{(1,8)}$ = 9.55; P = 0.0149). Posthoc analysis revealed a significant increase at 30 dpi (**; P < 0.01). **C)** There was no difference the in the total population of YFP+ Nestin+ GFAP+ RGLs. Error bars are SEM, n = 50+ YFP+ cells, n = 3 animals per group.

Discussion

The discovery of adult neurogenesis has garnered hope in developing new regenerative therapeutic interventions to combat neurodegenerative and other brain related diseases. More specifically efforts are being made to understand the cellular and molecular mechanisms that regulate the survival and development of NPCs in the adult brain given only 20% of newborn neurons survive to contribute functionally to neural networks (Kuhn et al., 2005; Sierra et al., 2010). This study contributes to this objective by examining the role of Beclin1 in adult hippocampal neurogenesis. Through creating an inducible Beclin1 nKO mouse model and using a retroviral-mediated gene transfer approach to specifically target the dividing NPCs we demonstrate Beclin1 is required for the generation and survival of adult-born neurons. These findings support other recent reports describing the essential role for autophagy in neurogenesis (Wang et al., 2013; McKnight et al., 2014; Yazdankhah et al., 2014), and extends our knowledge by examining the role of Beclin1 specifically in the formation of adult-generated neurons.

4.1 Removal of Beclin1 Reduces Adult Hippocampal Neurogenesis

Beclin1 has a cell-autonomous role in regulating adult hippocampal neurogenesis. This was evident by a reduction in the survival of Beclin1-null retroviral infected NPCs, and the reduction in the proportion and total population of proliferating cells, immature neurons and mature neurons in Beclin1 nKO mice. These results are consistent with, and expand upon recent findings by Yazdankhah et al. (2014) that demonstrate Beclin1 heterozygous knockout mice have a reduction in the proliferating and immature neuronal population. We extend these finding by showing Beclin1 is essential regulator of neurogenesis in the adult brain independent of its effects in the embryo. Our work also

analyzed the role of Beclin1 by specifically removing Beclin1 from SGZ neurogenic cells, whereas Yazdankhah et al. (2014) examined a knockout mouse model that had reduced levels of Beclin1 throughout the body and brain. Additionally, we find interesting differences in the results obtained from removing Beclin1 using a retroviral-mediated ablation model versus an inducible transgenic Beclin1 nKO mice model, which offers further insight into how Beclin1 regulates the different developmental subpopulations that comprise the dynamic process of adult neurogenesis.

4.2 Removal of Beclin1 Reduces the Survival of Immature and Adult-Generated Neurons

Retroviral-mediated removal of Beclin1 demonstrated a reduction in Beclin1-null NPCs compared to an internal RFP control virus. Since ratio analysis of surviving knockout versus control cells would account for the normal rate of cell death, this result suggests that removal of Beclin1 reduces the survival of proliferating NPCs. One possible method of confirming this interpretation is assessing whether Beclin1-null NPCs have a greater expression of apoptotic cell death markers, such as AC3 or terminaldeoxynucleotidyl transferase dUTP nick-end labelling (TUNEL). However, since expression of apoptotic cell markers is very transient (Kuhn et al., 2005), when combined with the sparse-labeling retroviral model, the population of co-labeled cells is too small to quantify. Instead of enhancing cell death, removal of Beclin1 could also reduce proliferation or maturation of NPCs, resulting in the downstream reduction of the total Beclin1-null NPC population. These possibilities warranted further investigation in our retroviral model, as well as in our inducible Beclin1 nKO model.

Surprisingly, we observed no change in the proportion of adult-generated neurons after retroviral-mediated removal of Beclin1. This was in contrast to the Beclin1 nKO mouse that had a significant reduction in the proportion and total population of immature and adult-generated neurons. This discrepancy may be attributed to differences in the total number of NPCs and/or the NPC subpopulation targeted for Beclin1 removal in the retroviral infected mice compared to the Beclin1 nKO mice.

In terms of the number of cells infected, the inducible nestin nKO mice target a larger (~65%) proportion of the NPCs compared to the sparse infection rate (~1%) of the NPCs targeted by a retroviral strategy (van Praag et al., 2002; Imayoshi et al., 2008). One confounding variable with targeting such a large population of cells in the Beclin1 nKO mouse model is that additional extrinsic effects can occur from mature Beclin1-null adult-generated neurons, influencing the subsequent developing NPCs. In contrast, the sparse labeling provided by retroviral mediate gene transfer would only produce a cell-autonomous effect. This suggests that Beclin1 may regulate NPC survival cell-autonomously in both the ablation models, however, in the Beclin1 nKO mouse there may be additional extrinsic regulation of NPC development. Our analysis of the total YFP+ Beclin1-null immature neurons versus the absolute population immature neurons in the Beclin1 nKO SGZ provides insight into possible extrinsic regulation by Beclin1. If Beclin1 had an additional extrinsic function, we would expect Beclin1-expressing immature neurons to also be reduced in the SGZ of Beclin1 nKO mice. Instead, the reduction in the absolute immature neuron population (Figure 13B) is similar to the reduction in the total YFP+ Beclin1-null immature neurons (Figure 12C), thus suggesting Beclin1 does not have an extrinsic role. Therefore, the difference in proportions of

Beclin1-null immature and mature neurons between ablation models does not appear to be regulated by the difference in overall number of Beclin1-null cells.

A more likely explanation for this discrepancy between ablation models is differences in NPC subpopulation targeted for Beclin1 removal. Retroviral-mediated gene transfer occurs in proliferating NPCs, and thus IPCs (type-2a to type-3) are the cells predominantly infected as published previously (van Praag et al., 2002; Jagasia et al., 2009) and confirmed in our laboratory. Alternatively, the Beclin1 nKO mouse model removes Beclin1 from nestin-expressing NPCs, including the RGL stem cell population and type-2a IPCs (Imayoshi et al., 2008). In this context, the reduction in the development of Beclin1-null immature and mature neurons in the Beclin1 nKO mouse may be attributed to an additional role of Beclin1 in the RGL stem cells and type-2a IPCs. In the proliferating IPCs, Beclin1 may only promote survival in the absence of reducing the proportion of neurons since IPCs are already proliferative and lineage-determined (Filippov et al., 2003). However, in the Beclin1 nKO mice, the removal of Beclin1 from RGLs could result in an IPC survival deficit, as well as an additional reduction in the proportion of proliferating NPCs and adult-generated neurons. One way to explore this hypothesize would be to examine the role of Beclin1 in RGLs.

4.3 A Possible Role for Beclin1 in Radial-Glia Like Stem Cells

There was an increase in the proportion of Beclin1-null RGL stem cells at one-month in the Beclin1 nKO mouse. This was surprising given that there was an overall reduction in neurogenesis. One simple explanation for this result is that the increase in proportion of Beclin1-null RGLs may be attributed to the relative decrease in the proportion of proliferating and immature neurons. This would suggest that removal of Beclin1 does

not impact the RGLs, but instead reduces proliferation of NPCs resulting in less IPCs and immature neurons, and consequently a higher proportion of RGL stem cells. In agreement with this hypothesis, there was no significant difference in the total population of YFP+ RGLs in the Beclin1 nKO mice at one-month post Beclin1 ablation, suggesting that the number of RGL stem cells is not increased. Furthermore, there is no change in the proportion of Beclin1 null RGLs at 14 dpi, instead the increase in proportion occurs at 30 dpi when there is also a reduction the proportion of proliferating NPCs and adult-generated neurons. Together these findings suggest that Beclin1 removal does not alter the RGL stem cells.

A second possibility is that removal of Beclin1 increases RGL quiescence. In this context, the expected result would be a depletion of the proliferating IPC population, followed by a substantial reduction in immature neurons, without a change in the total population of RGLs. In agreement, in the Beclin1 nKO mice we observed a reduction in the proportion of Beclin1 null proliferating cells at 14 dpi, followed by a reduction of immature neurons at 30 dpi, and no significant difference in the total population of RGLs.

A third interpretation of the results could be that Beclin1 removal increases the RGL stem cells. Although there was no significant difference in the total population of Beclin1-null RGLs, there was a noticeable trend towards an increase one-moth post Beclin1 ablation. Thus, it is possible that Beclin1 is important in maintenance of the RGL cells through changing the ratio of symmetric versus asymmetric divisions or altering the number of RGLs that are quiescent versus active to increase the number stem cells. One possibility is that the reduction in adult neurogenesis could have created extrinsic feedback to upregulate the population of RGLs as a compensatory mechanism. For instance, IPCs are

in close contact and can communicate with RGLs through GABA secretion (Miller and Gauthier-Fisher, 2009). As a result, IPCs could theoretically upregulate RGL symmetric division and self-renewal to expand the stem cell pool. The timeline of our results also supports this hypothesis with a reduction in the proportion of YFP+ proliferating cells at 14 dpi, followed by an increase in the proportion of YFP+ RGLs at 30 dpi in the Beclin1 nKO mice. Additionally, analysis of YFP+ RGLs at two-months post Beclin1 removal would help to clarify whether the total population of YFP+ RGLs is indeed being upregulated.

In order to help determine if Beclin1 has a cell-autonomous role in RGLs, ongoing work is examining the role of Beclin1-null RGLs *in vitro*. Preliminary neurosphere studies are ongoing using FACS sorted YFP+ NPCs from the Beclin1 nKO and WT mice. If Beclin1-removal triggers quiescence, we expect a reduction in the total number of neurospheres. Alternatively, if Beclin1 regulates proliferation, we expect smaller neurospheres. Cultured neurospheres have also been demonstrated to contain a large proportion of type-2 IPCs, astrocytes, and oligodendrocytes (Palmer et al., 1997). Therefore, to delineate the role of Beclin1 in both the RGL and type-2 IPC populations, analyses of both the RGL stem cells and IPCs will be further described using immunocytochemistry.

In summary, our results obtained to date suggest that there is either no change, or a possible increase in the stem cell pool. If we confirm that removal of Beclin1 increases the number of RGL cells, this would oppose the results of Wang et al. (2013) who report a reduction in the stem cell pool after embryonic deletion of the autophagy inducer FIP200 in GFAP expressing cells. In addition, they find that FIP200 ablation from

GFAP-expressing cells increases the production of astrocytes from adult neural stem cells, thereby altering RGL fate decisions from neurogenesis to astrogenesis. Other reports have demonstrated that RGLs can differentiate into post-mitotic astroglia resulting in depletion of the stem cell pool (Brunne et al., 2010; Bonaguidi et al., 2011; Encinas et al., 2011). However, this does not agree with our findings, since we observe an increase in proportion of Beclin1-null RGLs and not an increase in Beclin1-null GFAP+ cells that were nestin negative. Therefore our results suggest that Beclin1 removal from RGLs does not alter cell fate. The discrepancy between our results and Wang et al. (2013) may be due to three possibilities. First, FIP200 and Beclin1 have differential roles in regulating adult hippocampal neurogenesis. Second, removing autophagy from GFAP-expressing cells versus nestin-expressing NPCs ultimately ablates the process in different cell populations. For instance, GFAP is additionally expressed mature astrocytes (Figure 1), and therefore the discrepancy could be due to additive effects of autophagy ablation in astrocytes, which are an important component of the neurogenic niche and have been shown to regulate adult neurogenesis (Aimone et al., 2014). A third explanation is that Wang et al. (2013) ablate FIP200 during embryonic development, whereas we ablate Beclin1 in the adult animal for the purpose of examining neurogenesis in the adult context. Considering neurogenesis regulators can play different roles in embryonic versus adult neurogenesis (Urban and Guillemot, 2014), the discrepancy between our results may highlight differential roles of autophagy in embryonic versus adult neurogenesis.

4.4 Beclin1 Reduces the Number of Dividing NPCs

One of the most striking findings from the Beclin1 nKO mouse is the reduction in Beclin1-null proliferating NPCs. This is supported by a decline in the proportion of proliferating IPCs at 14 dpi irrespective of DCX expression, and a reduction in the total Beclin1-null proliferating population by 30 dpi, demonstrating Beclin1 has an overall effect of reducing proliferation. Additionally, there was greater ~3-fold reduction in Beclin1-null immature neurons compared to the ~2-fold reduction in Beclin1-null proliferating cells at one-month post Beclin1 ablation. Since one IPC undergoes many rounds of cell division and can produce multiple immature neurons, a more substantial loss in the immature neuron population compared to the proliferating population is suggestive of decreased production rather than cell death. In agreement, we did not see an increase in cells that expressed the apoptotic marker AC3 over time in the Beclin1 nKO mice. Overall, this data suggests Beclin1 reduces NPC proliferation contributing to the downstream effect of a reduction in the number of immature and mature neurons over time.

A potential caveat to the interpretation that Beclin1 is essential for proliferation of NPCs is that retroviral-mediated removal of Beclin1 from the dividing NPCs reduced cell survival without changing number of proliferating NPCs. Although we did not analyze the proportion of Beclin1-null proliferating NPCs, the proportion of proliferating Beclin1-null cells is not expected to be altered since there was no difference in the total number of Beclin1-null NPCs at two-weeks post Beclin1 removal. To verify this, ongoing work is confirming the number of proliferating Beclin1-null infected cells. If we find no difference in number of proliferating Beclin1-null infected cells this would raise a

discrepancy between our retroviral and nKO model. As discussed above this difference in effect on proliferation could be insightful and may be attributed to an alternative role for Beclin1 in different developmental subpopulations of NPCs. Since IPCs are already proliferating and lineage-determined at the time of retroviral infection, Beclin1 could only have a role in promoting survival. Whereas in the Beclin1 nKO mouse, Beclin1 is removed from the RGL stem cells and proliferating NPCs resulting in a dramatic reduction in proliferating NPCs.

The role of Beclin1 in reducing proliferation is in agreement with its well-established role as a tumor suppressor (Yue et al., 2003; Funderburk et al., 2010). Recently c-Myc activity has been reported by Cianfanelli et al. (2015) to be one mechanism by which Beclin1 may regulate cell proliferation. This report demonstrates that Beclin1 indirectly regulates c-Myc activity, a transcription factor involved in cell-cycle progression (Bretones et al., 2015), through the epidermal growth factor receptor (EGFR) pathway. Interestingly, c-Myc is phosphorylated upon EGFR activation by the ERK1/2 kinases to promote cell-cycle progression, and EGRF can activity be modulated by Beclin1-PI(3)K mediated endocytosis (Thoresen et al., 2010; Wei et al., 2013). As a result, siRNA knockdown of Beclin1 increased the amount of phosphorylated c-Myc. These findings were all obtained in HEK293 cancer cells, leaving it open to discovery if c-Myc is also responsible for the reduction in proliferating occurring during adult neurogenesis. To investigate this, YFP+ NPCs could be FACS sorted from Beclin1 nKO and WT controls, and the expression levels of c-Myc, its activated form phosphorylated c-Myc, EGFR, and ERK1/2 kinases, could be assessed by western blot. Therefore, our experiments could

probe if the reduction in proliferation of Beclin1-null cells could be rescued by targeting the c-Myc pathway.

4.5 Is Beclin1's Role in Adult Neurogenesis Autophagy Mediated?

An important question not addressed by this thesis is whether Beclin1's regulation of adult hippocampal neurogenesis is autophagy dependent or autophagy independent. Beclin1 has well-established role in autophagy induction and autophagosome formation (Liang et al., 1999; Kihara et al., 2001), and thus Beclin1 removal from NPCs likely reduces autophagy. In addition, Beclin1 has autophagy independent roles in diverse biological processes including endocytosis, phagocytosis, cytokinesis, and immunity (Funderburk et al., 2010; Wirawan et al., 2012). Yazdankhah et al. (2014), who in agreement with our results demonstrated that Beclin1 heterozygosis reduces the proliferating and immature neuron population of the adult SVZ, showed that Beclin1 heterozygosis reduces autophagy in neurospheres cultivated from adult SVZ NPCs. This suggests Beclin1 induces autophagy in adult NPCs *in vitro*, however, it is important to verify that Beclin1 removal from NPCs disrupts autophagy *in vivo*. In order to address this question, ongoing work is FACS sorting YFP+ NPCs from Beclin1 nKO and WT animals, and comparing the expression levels of autophagic markers, including LC3I, LC3II, and P62 by western blot analysis (Mizushima and Komatsu, 2011). If there is no difference in the expression of autophagic markers, this would suggest that Beclin1 is not required for autophagy induction in adult NPCs *in vivo*, and Beclin1 regulates adult neurogenesis via an autophagy independent mechanisms.

Conclusion

Using two different *in vivo* knockout strategies, our findings demonstrate that Beclin1 regulates NPC survival, proliferation, and development in the absence of changing fate, to ultimately regulate adult hippocampal neurogenesis. Moreover, we demonstrate Beclin1 expression in neurospheres cultured from adult NPCs and suggests a role for Beclin1 in regulating RGL stem cells. Further investigation into whether Beclin1's regulation of adult neurogenesis is autophagy mediated will advance knowledge of mechanisms that regulate NPC survival and maturation, and thus contribute to the field of regenerative medicine.

References

Aimone JB, Li Y, Lee SW, Clemenson GD, Deng W, Gage FH (2014) Regulation and function of adult neurogenesis: from genes to cognition. Physiol Rev 94:991-1026.

Aita VM, Liang XH, Murty VV, Pincus DL, Yu W, Cayanis E, Kalachikov S, Gilliam TC, Levine B (1999) Cloning and genomic organization of beclin 1, a candidate tumor suppressor gene on chromosome 17q21. Genomics 59:59-65.

Alirezaei M, Kemball CC, Flynn CT, Wood MR, Whitton JL, Kiosses WB (2010) Short-term fasting induces profound neuronal autophagy. Autophagy 6:702-710.

Altman J (1962) Are new neurons formed in the brains of adult mammals? Science 135:1127-1128.

Altman J (1969) Autoradiographic and histological studies of postnatal neurogenesis. IV. Cell proliferation and migration in the anterior forebrain, with special reference to persisting neurogenesis in the olfactory bulb. J Comp Neurol 137:433-457.

Altman J, Das GD (1965) Autoradiographic and histological evidence of postnatal hippocampal neurogenesis in rats. J Comp Neurol 124:319-335.

Babu H, Claasen JH, Kannan S, Runker AE, Palmer T, Kempermann G (2011) A protocol for isolation and enriched monolayer cultivation of neural precursor cells from mouse dentate gyrus. Front Neurosci 5:89.

Bonaguidi MA, Song J, Ming GL, Song H (2012) A unifying hypothesis on mammalian neural stem cell properties in the adult hippocampus. Curr Opin Neurobiol 22:754-761.

Bonaguidi MA, Wheeler MA, Shapiro JS, Stadel RP, Sun GJ, Ming GL, Song H (2011) In vivo clonal analysis reveals self-renewing and multipotent adult neural stem cell characteristics. In: Cell, pp 1142-1155. United States: 2011 Elsevier Inc.

Boya P, Reggiori F, Codogno P (2013) Emerging regulation and functions of autophagy. Nat Cell Biol 15:713-720.

Brandt MD, Jessberger S, Steiner B, Kronenberg G, Reuter K, Bick-Sander A, von der Behrens W, Kempermann G (2003) Transient calretinin expression defines early postmitotic step of neuronal differentiation in adult hippocampal neurogenesis of mice. Mol Cell Neurosci 24:603-613.

Bretones G, Delgado MD, Leon J (2015) Myc and cell cycle control. Biochim Biophys Acta 1849:506-516.

Brown JP, Couillard-Despres S, Cooper-Kuhn CM, Winkler J, Aigner L, Kuhn HG (2003) Transient expression of doublecortin during adult neurogenesis. J Comp Neurol 467:1-10.

Brunne B, Zhao S, Derouiche A, Herz J, May P, Frotscher M, Bock HH (2010) Origin, maturation, and astroglial transformation of secondary radial glial cells in the developing dentate gyrus. Glia 58:1553-1569.

Christian KM, Song H, Ming GL (2014) Functions and dysfunctions of adult hippocampal neurogenesis. Annu Rev Neurosci 37:243-262.

Cianfanelli V, D'Orazio M, Cecconi F (2015) AMBRA1 and BECLIN 1 interplay in the crosstalk between autophagy and cell proliferation. Cell Cycle 14:959-963.

Dhaliwal J, Lagace DC (2011) Visualization and genetic manipulation of adult neurogenesis using transgenic mice. Eur J Neurosci 33:1025-1036.

Di Bartolomeo S, Nazio F, Cecconi F (2010) The role of autophagy during development in higher eukaryotes. Traffic 11:1280-1289.

Djavaheri-Mergny M, Maiuri MC, Kroemer G (2010) Cross talk between apoptosis and autophagy by caspase-mediated cleavage of Beclin 1. Oncogene 29:1717-1719.

Duan X, Kang E, Liu CY, Ming GL, Song H (2008) Development of neural stem cell in the adult brain. Curr Opin Neurobiol 18:108-115.

Encinas JM, Michurina TV, Peunova N, Park JH, Tordo J, Peterson DA, Fishell G, Koulakov A, Enikolopov G (2011) Division-coupled astrocytic differentiation and age-related depletion of neural stem cells in the adult hippocampus. Cell Stem Cell 8:566-579.

Eriksson PS, Perfilieva E, Bjork-Eriksson T, Alborn AM, Nordborg C, Peterson DA, Gage FH (1998) Neurogenesis in the adult human hippocampus. Nat Med 4:1313-1317.

Filippov V, Kronenberg G, Pivneva T, Reuter K, Steiner B, Wang LP, Yamaguchi M, Kettenmann H, Kempermann G (2003) Subpopulation of nestin-expressing progenitor cells in the adult murine hippocampus shows electrophysiological and morphological characteristics of astrocytes. Mol Cell Neurosci 23:373-382.

Fimia GM, Stoykova A, Romagnoli A, Giunta L, Di Bartolomeo S, Nardacci R, Corazzari M, Fuoco C, Ucar A, Schwartz P, Gruss P, Piacentini M, Chowdhury K, Cecconi F (2007) Ambra1 regulates autophagy and development of the nervous system. Nature 447:1121-1125.

Funderburk SF, Wang QJ, Yue Z (2010) The Beclin 1-VPS34 complex--at the crossroads of autophagy and beyond. Trends Cell Biol 20:355-362.

Garcia AD, Doan NB, Imura T, Bush TG, Sofroniew MV (2004) GFAP-expressing progenitors are the principal source of constitutive neurogenesis in adult mouse forebrain. In: Nat Neurosci, pp 1233-1241. United States.

Gordy C, He YW (2012) The crosstalk between autophagy and apoptosis: where does this lead? Protein & cell 3:17-27.

Gross CG (2000) Neurogenesis in the adult brain: death of a dogma. Nat Rev Neurosci 1:67-73.

Hara T, Nakamura K, Matsui M, Yamamoto A, Nakahara Y, Suzuki-Migishima R, Yokoyama M, Mishima K, Saito I, Okano H, Mizushima N (2006) Suppression of basal autophagy in neural cells causes neurodegenerative disease in mice. Nature 441:885-889.

He C, Levine B (2010) The Beclin 1 interactome. Curr Opin Cell Biol 22:140-149.

Hendrickson ML, Rao AJ, Demerdash ON, Kalil RE (2011) Expression of nestin by neural cells in the adult rat and human brain. PLoS One 6:e18535.

Hsieh J (2012) Orchestrating transcriptional control of adult neurogenesis. Genes Dev 26:1010-1021.

Imayoshi I, Ohtsuka T, Metzger D, Chambon P, Kageyama R (2006) Temporal regulation of Cre recombinase activity in neural stem cells. Genesis 44:233-238.

Imayoshi I, Sakamoto M, Ohtsuka T, Takao K, Miyakawa T, Yamaguchi M, Mori K, Ikeda T, Itohara S, Kageyama R (2008) Roles of continuous neurogenesis in the structural and functional integrity of the adult forebrain. Nat Neurosci 11:1153-1161.

Itakura E, Kishi C, Inoue K, Mizushima N (2008) Beclin 1 forms two distinct phosphatidylinositol 3-kinase complexes with mammalian Atg14 and UVRAG. Mol Biol Cell 19:5360-5372.

Jagasia R, Steib K, Englberger E, Herold S, Faus-Kessler T, Saxe M, Gage FH, Song H, Lie DC (2009) GABA-cAMP response element-binding protein signaling regulates maturation and survival of newly generated neurons in the adult hippocampus. J Neurosci 29:7966-7977.

Kaplan MS (2001) Environment complexity stimulates visual cortex neurogenesis: death of a dogma and a research career. Trends Neurosci 24:617-620.

Kaushik S, Rodriguez-Navarro JA, Arias E, Kiffin R, Sahu S, Schwartz GJ, Cuervo AM, Singh R (2011) Autophagy in hypothalamic AgRP neurons regulates food intake and energy balance. In: Cell Metab, pp 173-183. United States: 2011 Elsevier Inc.

Kempermann G, Kuhn HG, Gage FH (1997) More hippocampal neurons in adult mice living in an enriched environment. Nature 386:493-495.

Kempermann G, Jessberger S, Steiner B, Kronenberg G (2004) Milestones of neuronal development in the adult hippocampus. Trends Neurosci 27:447-452.

Kihara A, Kabeya Y, Ohsumi Y, Yoshimori T (2001) Beclin-phosphatidylinositol 3-kinase complex functions at the trans-Golgi network. EMBO Rep 2:330-335.

Komatsu M, Wang QJ, Holstein GR, Friedrich VL, Jr., Iwata J, Kominami E, Chait BT, Tanaka K, Yue Z (2007) Essential role for autophagy protein Atg7 in the maintenance of axonal homeostasis and the prevention of axonal degeneration. Proc Natl Acad Sci U S A 104:14489-14494.

Komatsu M, Waguri S, Chiba T, Murata S, Iwata J, Tanida I, Ueno T, Koike M, Uchiyama Y, Kominami E, Tanaka K (2006) Loss of autophagy in the central nervous system causes neurodegeneration in mice. Nature 441:880-884.

Kronenberg G, Reuter K, Steiner B, Brandt MD, Jessberger S, Yamaguchi M, Kempermann G (2003) Subpopulations of proliferating cells of the adult hippocampus respond differently to physiologic neurogenic stimuli. J Comp Neurol 467:455-463.

Kuhn HG, Dickinson-Anson H, Gage FH (1996) Neurogenesis in the dentate gyrus of the adult rat: age-related decrease of neuronal progenitor proliferation. J Neurosci 16:2027-2033.

Kuhn HG, Biebl M, Wilhelm D, Li M, Friedlander RM, Winkler J (2005) Increased generation of granule cells in adult Bcl-2-overexpressing mice: a role for cell death during continued hippocampal neurogenesis. Eur J Neurosci 22:1907-1915.

Kuma A, Hatano M, Matsui M, Yamamoto A, Nakaya H, Yoshimori T, Ohsumi Y, Tokuhisa T, Mizushima N (2004) The role of autophagy during the early neonatal starvation period. Nature 432:1032-1036.

Lagace DC, Donovan MH, DeCarolis NA, Farnbauch LA, Malhotra S, Berton O, Nestler EJ, Krishnan V, Eisch AJ (2010) Adult hippocampal neurogenesis is functionally important for stress-induced social avoidance. Proc Natl Acad Sci U S A 107:4436-4441.

Lagace DC, Whitman MC, Noonan MA, Ables JL, DeCarolis NA, Arguello AA, Donovan MH, Fischer SJ, Farnbauch LA, Beech RD, DiLeone RJ, Greer CA, Mandyam CD, Eisch AJ (2007) Dynamic contribution of nestin-expressing stem cells to adult neurogenesis. J Neurosci 27:12623-12629.

Lendahl U, Zimmerman LB, McKay RD (1990) CNS stem cells express a new class of intermediate filament protein. In: Cell, pp 585-595. United States.

Liang XH, Jackson S, Seaman M, Brown K, Kempkes B, Hibshoosh H, Levine B (1999) Induction of autophagy and inhibition of tumorigenesis by beclin 1. Nature 402:672-676.

Liang XH, Kleeman LK, Jiang HH, Gordon G, Goldman JE, Berry G, Herman B, Levine B (1998) Protection against fatal Sindbis virus encephalitis by beclin, a novel Bcl-2-interacting protein. J Virol 72:8586-8596.

Lugert S, Basak O, Knuckles P, Haussler U, Fabel K, Gotz M, Haas CA, Kempermann G, Taylor V, Giachino C (2010) Quiescent and active hippocampal neural stem cells with distinct morphologies respond selectively to physiological and pathological stimuli and aging. Cell Stem Cell 6:445-456.

Lv X, Jiang H, Li B, Liang Q, Wang S, Zhao Q, Jiao J (2014) The crucial role of Atg5 in cortical neurogenesis during early brain development. Sci Rep 4:6010.

Ma DK, Bonaguidi MA, Ming GL, Song H (2009) Adult neural stem cells in the mammalian central nervous system. Cell Res 19:672-682.

Macintosh RL, Ryan KM (2013) Autophagy in tumour cell death. Seminars in cancer biology.

Maiuri MC, Zalckvar E, Kimchi A, Kroemer G (2007) Self-eating and self-killing: crosstalk between autophagy and apoptosis. Nat Rev Mol Cell Biol 8:741-752.

Mandyam CD, Harburg GC, Eisch AJ (2007) Determination of key aspects of precursor cell proliferation, cell cycle length and kinetics in the adult mouse subgranular zone. Neuroscience 146:108-122.

McKnight NC, Zhong Y, Wold MS, Gong S, Phillips GR, Dou Z, Zhao Y, Heintz N, Zong WX, Yue Z (2014) Beclin 1 is required for neuron viability and regulates endosome pathways via the UVRAG-VPS34 complex. PLoS Genet 10:e1004626.

Miller FD, Gauthier-Fisher A (2009) Home at last: neural stem cell niches defined. Cell Stem Cell 4:507-510.

Ming GL, Song H (2011) Adult neurogenesis in the mammalian brain: significant answers and significant questions. Neuron 70:687-702.

Mizushima N, Komatsu M (2011) Autophagy: renovation of cells and tissues. Cell 147:728-741.

Palmer TD, Takahashi J, Gage FH (1997) The adult rat hippocampus contains primordial neural stem cells. Mol Cell Neurosci 8:389-404.

Pattingre S, Tassa A, Qu X, Garuti R, Liang XH, Mizushima N, Packer M, Schneider MD, Levine B (2005) Bcl-2 antiapoptotic proteins inhibit Beclin 1-dependent autophagy. Cell 122:927-939.

Petiot A, Ogier-Denis E, Blommaart EF, Meijer AJ, Codogno P (2000) Distinct classes of phosphatidylinositol 3'-kinases are involved in signaling pathways that control macroautophagy in HT-29 cells. J Biol Chem 275:992-998.

Phadwal K, Watson AS, Simon AK (2013) Tightrope act: autophagy in stem cell renewal, differentiation, proliferation, and aging. Cell Mol Life Sci 70:89-103.

Proenca CC, Stoehr N, Bernhard M, Seger S, Genoud C, Roscic A, Paganetti P, Liu S, Murphy LO, Kuhn R, Bouwmeester T, Galimberti I (2013) Atg4b-dependent autophagic flux alleviates Huntington's disease progression. PLoS One 8:e68357.

Qu X, Yu J, Bhagat G, Furuya N, Hibshoosh H, Troxel A, Rosen J, Eskelinen EL, Mizushima N, Ohsumi Y, Cattoretti G, Levine B (2003) Promotion of tumorigenesis by heterozygous disruption of the beclin 1 autophagy gene. J Clin Invest 112:1809-1820.

Sierra A, Encinas JM, Deudero JJ, Chancey JH, Enikolopov G, Overstreet-Wadiche LS, Tsirka SE, Maletic-Savatic M (2010) Microglia shape adult hippocampal neurogenesis through apoptosis-coupled phagocytosis. Cell Stem Cell 7:483-495.

Song J, Zhong C, Bonaguidi MA, Sun GJ, Hsu D, Gu Y, Meletis K, Huang ZJ, Ge S, Enikolopov G, Deisseroth K, Luscher B, Christian KM, Ming GL, Song H (2012) Neuronal circuitry mechanism regulating adult quiescent neural stem-cell fate decision. In: Nature, pp 150-154. England.

Srinivas S, Watanabe T, Lin CS, William CM, Tanabe Y, Jessell TM, Costantini F (2001) Cre reporter strains produced by targeted insertion of EYFP and ECFP into the ROSA26 locus. BMC Dev Biol 1:4.

Suh H, Consiglio A, Ray J, Sawai T, D'Amour KA, Gage FH (2007) In vivo fate analysis reveals the multipotent and self-renewal capacities of Sox2+ neural stem cells in the adult hippocampus. Cell Stem Cell 1:515-528.

Tang G, Gudsnuk K, Kuo SH, Cotrina ML, Rosoklija G, Sosunov A, Sonders MS, Kanter E, Castagna C, Yamamoto A, Yue Z, Arancio O, Peterson BS, Champagne F, Dwork AJ, Goldman J, Sulzer D (2014) Loss of mTOR-dependent macroautophagy causes autistic-like synaptic pruning deficits. Neuron 83:1131-1143.

Tashiro A, Zhao C, Gage FH (2006a) Retrovirus-mediated single-cell gene knockout technique in adult newborn neurons in vivo. In: Nat Protoc, pp 3049-3055. England.

Tashiro A, Makino H, Gage FH (2007) Experience-specific functional modification of the dentate gyrus through adult neurogenesis: a critical period during an immature stage. J Neurosci 27:3252-3259.

Tashiro A, Sandler VM, Toni N, Zhao C, Gage FH (2006b) NMDA-receptor-mediated, cell-specific integration of new neurons in adult dentate gyrus. Nature 442:929-933.

Thoresen SB, Pedersen NM, Liestol K, Stenmark H (2010) A phosphatidylinositol 3-kinase class III sub-complex containing VPS15, VPS34, Beclin 1, UVRAG and BIF-1 regulates cytokinesis and degradative endocytic traffic. Exp Cell Res 316:3368-3378.

Truett GE, Heeger P, Mynatt RL, Truett AA, Walker JA, Warman ML (2000) Preparation of PCR-quality mouse genomic DNA with hot sodium hydroxide and tris (HotSHOT). Biotechniques 29:52, 54.

Tsukamoto S, Kuma A, Murakami M, Kishi C, Yamamoto A, Mizushima N (2008) Autophagy is essential for preimplantation development of mouse embryos. Science 321:117-120.

Urban N, Guillemot F (2014) Neurogenesis in the embryonic and adult brain: same regulators, different roles. Front Cell Neurosci 8:396.

van Praag H, Kempermann G, Gage FH (1999) Running increases cell proliferation and neurogenesis in the adult mouse dentate gyrus. Nat Neurosci 2:266-270.

van Praag H, Schinder AF, Christie BR, Toni N, Palmer TD, Gage FH (2002) Functional neurogenesis in the adult hippocampus. Nature 415:1030-1034.

Vazquez P, Arroba AI, Cecconi F, de la Rosa EJ, Boya P, de Pablo F (2012) Atg5 and Ambra1 differentially modulate neurogenesis in neural stem cells. Autophagy 8:187-199.

Wang C, Liang CC, Bian ZC, Zhu Y, Guan JL (2013) FIP200 is required for maintenance and differentiation of postnatal neural stem cells. Nat Neurosci 16:532-542.

Wei Y, Sinha S, Levine B (2008) Dual role of JNK1-mediated phosphorylation of Bcl-2 in autophagy and apoptosis regulation. Autophagy 4:949-951.

Wei Y, Zou Z, Becker N, Anderson M, Sumpter R, Xiao G, Kinch L, Koduru P, Christudass CS, Veltri RW, Grishin NV, Peyton M, Minna J, Bhagat G, Levine B (2013) EGFR-mediated Beclin 1 phosphorylation in autophagy suppression, tumor progression, and tumor chemoresistance. Cell 154:1269-1284.

Wirawan E, Lippens S, Vanden Berghe T, Romagnoli A, Fimia GM, Piacentini M, Vandenabeele P (2012) Beclin1: a role in membrane dynamics and beyond. Autophagy 8:6-17.

Wirawan E, Vande Walle L, Kersse K, Cornelis S, Claerhout S, Vanoverberghe I, Roelandt R, De Rycke R, Verspurten J, Declercq W, Agostinis P, Vanden Berghe T, Lippens S, Vandenabeele P (2010) Caspase-mediated cleavage of Beclin-1 inactivates Beclin-1-induced autophagy and enhances apoptosis by promoting the release of proapoptotic factors from mitochondria. Cell Death Dis 1:e18.

Xi Y, Dhaliwal J, Ceizar M, Vaculik M, Kumar KL, Snapyan M, Saghatelyan A, Lagace DC (2015) The Requirement of Autophagy-Related Gene 5 (ATG5) for Adult HIppocampal Neurogenesis. In: University of Ottawa.

Yamaguchi M, Saito H, Suzuki M, Mori K (2000) Visualization of neurogenesis in the central nervous system using nestin promoter-GFP transgenic mice. Neuroreport 11:1991-1996.

Yamamoto A, Yue Z (2014) Autophagy and its normal and pathogenic states in the brain. Annu Rev Neurosci 37:55-78.

Yao B, Jin P (2014) Unlocking epigenetic codes in neurogenesis. Genes Dev 28:1253-1271.

Yazdankhah M, Farioli-Vecchioli S, Tonchev AB, Stoykova A, Cecconi F (2014) The autophagy regulators Ambra1 and Beclin 1 are required for adult neurogenesis in the brain subventricular zone. Cell Death Dis 5:e1403.

Yue Z, Friedman L, Komatsu M, Tanaka K (2009) The cellular pathways of neuronal autophagy and their implication in neurodegenerative diseases. Biochim Biophys Acta 1793:1496-1507.

Yue Z, Jin S, Yang C, Levine AJ, Heintz N (2003) Beclin 1, an autophagy gene essential for early embryonic development, is a haploinsufficient tumor suppressor. Proc Natl Acad Sci U S A 100:15077-15082.

Zalckvar E, Berissi H, Eisenstein M, Kimchi A (2009) Phosphorylation of Beclin 1 by DAP-kinase promotes autophagy by weakening its interactions with Bcl-2 and Bcl-XL. Autophagy 5:720-722.

Zeng M, Zhou JN (2008) Roles of autophagy and mTOR signaling in neuronal differentiation of mouse neuroblastoma cells. Cell Signal 20:659-665.

Zhao C, Deng W, Gage FH (2008) Mechanisms and functional implications of adult neurogenesis. Cell 132:645-660.

Zhao C, Teng EM, Summers RG, Jr., Ming GL, Gage FH (2006) Distinct morphological stages of dentate granule neuron maturation in the adult mouse hippocampus. J Neurosci 26:3-11.